

TNF deficiency causes alterations in the spatial organization of neurogenic zones and alters the number of microglia and neurons in the cerebral cortex

Minna Yli-Karjanmaa^{a,1}, Kathrine Solevad Larsen^{a,1}, Christina Dühring Fenger^a, Lotte Kellemann Kristensen^a, Nellie Anne Martin^a, Peter Toft Jensen^a, Alexandre Breton^b, Lubov Nathanson^c, Pernille Vinther Nielsen^a, Minna Christiansen Lund^a, Stephanie Lindeman Carlsen^a, Jan Bert Gramsbergen^a, Bente Finsen^{a,d}, Jane Stubbe^e, Lars Henrik Frich^f, Helen Stolp^{b,g}, Roberta Brambilla^{a,d,h}, Daniel Clive Anthony^{a,b,d}, Morten Meyer^{a,d}, Kate Lykke Lambertsen^{a,d,i,*}

^a Department of Neurobiology Research, Institute of Molecular Medicine, University of Southern Denmark, Odense, Denmark

^b Department of Pharmacology, University of Oxford, Oxford, UK

^c Institute for Neuro Immune Medicine, Dr. Kiran C. Patel College of Osteopathic Medicine, Nova Southeastern University, Fort Lauderdale, FL, USA

^d BRIDGE – Brain Research – Inter-Disciplinary Guided Excellence, Department of Clinical Research, University of Southern Denmark, Odense, Denmark

^e Department of Cardiovascular and Renal Research, Institute of Molecular Medicine, University of Southern Denmark, Odense, Denmark

^f Orthopedic Research Unit, Department of Clinical Research, University of Southern Denmark, Odense, Denmark

^g Department of Comparative Biomedical Sciences, Royal Veterinary College, London, UK

^h The Miami Project to Cure Paralysis, Miller School of Medicine, University of Miami, Miami, FL, USA

ⁱ Department of Neurology, Odense University Hospital, Odense, Denmark

ARTICLE INFO

Keywords:

Cytokines
Neurogenesis
TNF inhibitors

ABSTRACT

Background: Although tumor necrosis factor (TNF) inhibitors are used to treat chronic inflammatory diseases, there is little information about how long-term inhibition of TNF affects the homeostatic functions that TNF maintains in the intact CNS.

Materials and methods: To assess whether developmental TNF deficiency causes alterations in the naïve CNS, we estimated the number of proliferating cells, microglia, and neurons in the developing neocortex of E13.5, P7 and adult TNF knock out ($\text{TNF}^{-/-}$) mice and wildtype (WT) littermates. We also measured changes in gene and protein expression and monoamine levels in adult WT and $\text{TNF}^{-/-}$ mice. To evaluate long-term effects of TNF inhibitors, we treated healthy adult C57BL/6 mice with either saline, the selective soluble TNF inhibitor XPro1595, or the nonselective TNF inhibitor etanercept. We estimated changes in cell number and protein expression after two months of treatment. We assessed the effects of TNF deficiency on cognition by testing adult

Abbreviations: AD, Alzheimer's disease; Alox-8, arachidonate 8-lipoxygenase; Asic1, Acid-sensing ion channel 1; BBB, Blood-brain barrier; BrdU, 5'-Bromo-2'-Deoxyuridine; CNS, central nervous system; Comt, catechol-O-methyltransferase; CTHRC1, Collagen Triple Helix Repeat Containing 1; DAB, 3,3'-Diaminobenzidine; DA, dopamine; DAPI, 4',6-diamidino-2-phenylindol; DCX, Doublecortin; DMEM, Dulbecco's Modified Eagle Medium; DOPAC, 3,4-dihydroxyphenylacetic acid; EdU, 5-ethynyl-2'-deoxyuridine; E, Embryonic day; FBS, foetal bovine serum; FDR, False discovery rate; FZD, Frizzled; GE, ganglionic eminence; GLUT1, Glucose transporter 1; GO, Gene Ontology; HBSS, Hanks' Balanced Salt Solution; HE, hematoxylin and eosin; 5-HIAA, 5-hydroxyindoleacetic acid; HPLC, High-performance liquid chromatography; HPRT1, hypoxanthine phosphoribosyltransferase 1; HRP, Horse-radish peroxidase; 5-HT, 5-hydroxytryptamine; 5-HTT, serotonin transporter; Htr2a, 5-hydroxytryptamine receptor 2a; HVA, homovanillic acid; IBD, inflammatory bowel disease; IL, Interleukin; Itpka, inositol-triphosphate 3-kinase; i.p., intraperitoneal; KEGG, Kyoto Encyclopaedia of Genes and Genomes; Lpl, lipoprotein lipase; LPS, lipopolysaccharide; MECP2, Methyl-CpG-binding protein 2; MS, multiple sclerosis; NA, noradrenalin; Nnt, nicotinamide nucleotide transhydrogenase; NF- κ B, Nuclear factor-kappa B; Park2, Parkin RBR E3 Ubiquitin Protein Ligase; P, Postnatal day; PBS, Phosphate-buffered saline; PCA, perchloric acid; PFA, Paraformaldehyde; RA, rheumatoid arthritis; RT-qPCR, Reverse transcriptase-quantitative polymerase chain reaction; SAM, Significance Analysis of Microarray; s.c., subcutaneous; SEZ, subependymal zone; Snca, Synuclein alpha; solTNF, Soluble TNF; SVZ, Subventricular zone; Tacr3, Tachykinin receptor 3; TB, Toluidine blue; TBST, Tris-buffered saline + Tween20; **TNF**, Tumor necrosis factor; tmTNF, Transmembrane TNF; TNFR1, TNF receptor 1; TNFR2, TNF receptor 2; VZ, ventricular zone; WT, wildtype

* Corresponding author at: Department of Neurobiology Research, Institute of Molecular Medicine, University of Southern Denmark, J.B. Winsloewsvej 21, st, DK-5000 Odense C, Denmark.

E-mail address: klambertsen@health.sdu.dk (K.L. Lambertsen).

¹ Equal contributors.

WT and TNF^{−/−} mice and mice treated with saline, XPro1595, or etanercept with specific behavioral tasks.

Results: TNF deficiency decreased the number of proliferating cells and microglia and increased the number of neurons. At the same time, TNF deficiency decreased the expression of WNT signaling-related proteins, specifically Collagen Triple Helix Repeat Containing 1 (CTHRC1) and Frizzled receptor 6 (FZD6). In contrast to XPro1595, long-term inhibition of TNF with etanercept in adult C57BL/6 mice decreased the number of BrdU⁺ cells in the granule cell layer of the dentate gyrus. Etanercept, but not XPro1595, also impaired spatial learning and memory in the Barnes maze memory test.

Conclusion: TNF deficiency impacts the organization of neurogenic zones and alters the cell composition in brain. Long-term inhibition of TNF with the nonselective TNF inhibitor etanercept, but not the soluble TNF inhibitor XPro1595, decreases neurogenesis in the adult mouse hippocampus and impairs learning and memory after two months of treatment.

1. Background

The cytokine tumor necrosis factor (TNF) plays important roles in the homeostasis of the healthy central nervous system (CNS), as well as in pathological inflammatory states. TNF is expressed as a transmembrane form (tmTNF) that can be cleaved into a soluble form (solTNF) by the TNF alpha converting enzyme (TACE/ADAM17) (Black et al., 1997). Signal transduction of solTNF mainly occurs through TNF receptor 1 (TNFR1), while tmTNF can activate both TNFR1 and TNFR2 (Grell et al., 1995; Grell et al., 1998). TNF signaling has been associated with neuron maturation in the dentate gyrus and the shaping of dendritic trees in CA1 and CA3 hippocampal regions in early development (Golan et al., 2004a). Signaling through TNFR1 can decrease neural progenitor proliferation in the granule cell layer of the dentate gyrus, increase apoptosis of neural stem cells, and disrupt their differentiation into neurons (Hofer et al., 2011; Iosif et al., 2006; Keohane et al., 2010; Seguin et al., 2009). In contrast, lack of TNF receptor 2 (TNFR2) can affect the formation of new neurons (Chen and Palmer, 2013), indicating that TNFR2 is important for neurogenesis. Although neurogenesis declines with age, it continues into adulthood in rodents (Bordiuk et al., 2014) and also moderately in humans (Altman and Das, 1965; Eriksson et al., 1998; Spalding et al., 2013).

In the healthy CNS, TNF is produced by microglia, astrocytes, and neurons (reviewed by (McCoy and Tansey, 2008)), while in inflammation it is mainly produced by microglia (reviewed in (Lambertsen et al., 2018)). Surveilling microglia are involved in clearing apoptotic newborn neurons, synaptic pruning, and enhancing neurogenesis (Batchelor et al., 2002; Paolicelli et al., 2011; Ribeiro Xavier et al., 2015; Schafer et al., 2012; Shigemoto-Mogami et al., 2014). On the other hand, activated microglia can impair integration of newborn neurons into the neural network (Belarbi et al., 2012), and in redundant inflammatory conditions they can exaggerate the death of newborn neurons by secreting neurotoxic proinflammatory cytokines like TNF, interleukin (IL)-6, and IL-1β (Cacci et al., 2005; Ekdahl et al., 2003; Monje et al., 2003). It is well established, however, that microglia can benefit neuron proliferation in both intact and inflamed CNS (Bachstetter et al., 2011; Butovsky et al., 2005; Ekdahl, 2012; Ekdahl et al., 2009; Hanisch and Kettenmann, 2007; Shigemoto-Mogami et al., 2014; Vukovic et al., 2012; Walton et al., 2006; Ziv et al., 2006; Aarum et al., 2003).

TNF signaling regulates cognition in adulthood by interfering with memory consolidation (Golan et al., 2004a). Elevated TNF levels cause depressive-like behavior in rodents while inhibition of solTNF with the selective solTNF inhibitor XPro1595 reverses the effects (Bedrosian et al., 2013; Kaster et al., 2012). Also, inhibition of TNF has been shown to relieve fatigue and symptoms of depression associated with chronic inflammatory diseases (Tyring et al., 2006).

The TNF inhibitors currently in use to treat chronic inflammatory diseases block both solTNF and tmTNF. Their beneficial effects are hampered by increased risk of infections, cardiovascular conditions, and demyelination (Scheinfeld, 2004). These negative side-effects have been associated with tmTNF inhibition as tmTNF supports secondary

lymphoid structure and promotes the normal function of the innate immune system (Ruuls et al., 2001), just as tmTNF appears to be important in cardiac remodeling (Danila et al., 2008) and remyelination (Brambilla et al., 2011). Selective solTNF inhibitors are being extensively studied in experimental CNS pathologies to find safer alternatives to existing TNF inhibitors without compromising the inflammation-suppressing effects (Barnum et al., 2014; Brambilla et al., 2011; Cavanagh et al., 2016; Clausen et al., 2014; Karamita et al., 2017; MacPherson et al., 2017; Novrup et al., 2014).

WNT signaling is a key regulator of embryonic neurogenesis (Kleber and Sommer, 2004) and is the main pathway in adult neurogenesis, synaptogenesis (Hall et al., 2000; Lie et al., 2005; Rosso and Inestrosa, 2013), and hippocampal function (Alvarez-Buylla and Lim, 2004). WNT proteins work through frizzled receptors (FZD) (Bhanot et al., 1996), of which FZD6 can activate the non-canonical/planar cell polarity pathway and inhibit the canonical pathway (Golan et al., 2004b; Mirkovic et al., 2011). Collagen Triple Helix Repeat Containing 1 (CTHRC1) is another WNT cofactor protein involved in activation of the planar cell polarity pathway (Yamamoto et al., 2008). Both FZD6 and CTHRC1 stabilize the WNT receptor complex (Yamamoto et al., 2008).

The aim of the present study was to explore the effects of TNF deficiency in the developing and adult cortex and hippocampus on the organization of neurogenic zones and on memory and learning. We also compared the effect on learning and memory of nonselective TNF inhibition using etanercept versus selective solTNF inhibition using XPro1595.

2. Materials and methods

2.1. Animals

TNF^{−/−} mice, on a C57BL/6 background (Pasparakis et al., 1996), were obtained from the Jackson Laboratory and transferred to the Biomedical Laboratory, University of Southern Denmark where they were kept as a colony. Experiments were performed using embryonic day 13.5 (E13.5), postnatal day 7 (P7), and male 2- or 4-month-old (adult) TNF^{−/−} mice and wildtype (WT) littermates, as well as 2-month-old C57BL/6 male mice (Taconic Ltd., Ry, Denmark), in the studies with TNF inhibitor treatments. The animals were housed in diurnal lighting conditions with food and water available *ad libitum*. Animal experiments were performed according to the guidelines and regulations approved by the Danish Animal Ethical Committee (numbers 2011/561-1950 and 2013-15-2934-00924).

2.2. Study design

We first characterized the possible effects of developmental TNF deficiency and long-term inhibition of TNF in adulthood on gene and protein expression, monoamine levels, neurogenesis, and cell composition in the brain, and on the function and permeability of the blood-brain barrier (BBB). We then investigated the effect of TNF deficiency on cognitive functions.

2.3. Pharmacological treatment

Saline, XPro1595 (10 mg/kg) (Xencor Inc., Monrovia, CA) (Steed et al., 2003), or etanercept (10 mg/kg) (Enbrel, Amgen-Wyeth, Thousand Oaks, CA, USA) was administered subcutaneously (s.c.) in the 2-month-old C57BL/6 mice every third day for two months. One day after the first s.c. injection of saline, XPro1595, or etanercept, a single injection of 5'-Bromo-2'-Deoxyuridine (BrdU) (50 mg/kg, Sigma-Aldrich, Søborg, Denmark) was administered intraperitoneally (i.p.). Seven (7) weeks later, just prior to the Barnes maze test and one week prior to euthanization, mice were administered i.p. with a single injection of 5-ethynyl-2'-deoxyuridine (EdU) (50 mg/kg, InVitrogen, Tåstrup, Denmark). Mice were weighed every third day, starting on the day of the first saline, XPro1595, or etanercept injection.

2.4. Tissue processing

E13.5 WT and TNF^{-/-} fetuses were obtained after cervical dislocation of the dams. Whole fetal brains were fixed in Bouin's solution (Sigma-Aldrich, Denmark) before being rinsed, dehydrated in increasing concentrations of ethanol, and embedded in paraffin (Stolp et al., 2011). Coronal brain sections of 10 µm thicknesses were cut on a microtome.

P7 and adult mice were overdosed i.p. with pentobarbital (200 mg/ml) containing lidocainhydrochlorid (20 mg/ml) (Glostrup Apotek, Glostrup, Denmark) and perfused through the left ventricle with ice-cold phosphate-buffered saline (PBS, pH 7.4, Sigma-Aldrich) followed by ice-cold 4% paraformaldehyde (PFA, pH 7.4, Sigma-Aldrich). Brains from P7 mice were paraffin-embedded and cut into 6 parallel series of

30 µm thick microtome sections. Brains from adult mice were cut on a vibratome into 60 µm free-floating coronal sections in 6 parallel series, stored in de Olmos cryoprotectant solution containing 1% polyvinylpyrrolidone and 20% sucrose diluted in a mixture of 30% ethylene glycol and PBS, and stored in a freezer at -12 °C until further processing.

PBS-perfused brains of 2-month-old WT and TNF^{-/-} male mice were dissected and processed for monoamine analysis or microarray and real-time reverse transcriptase-quantitative polymerase chain reaction (RT-qPCR) analysis. PBS-perfused brains from 4-month-old WT and TNF^{-/-} mice and saline-, XPro1595-, and etanercept-treated C57BL/6 mice were divided into left and right hemispheres and stored at -80 °C before processing for Western blotting. Blood from mice treated with saline or TNF inhibitors was collected in EDTA-coated Eppendorf tubes and centrifuged 20 min at 3,000g, 4 °C. Plasma was stored at -80 °C until processing for Multiplex cytokine assay (Mesoscale Discovery, Rockville, MD, USA) as previously described (Madsen et al., 2016).

2.5. Microarray procedure and analysis

Two-months old, adult male WT and TNF^{-/-} brain lysates were used for RNA isolation. Isolated RNA was quality assessed using the Agilent RNA 6000 Nano Kit (Agilent Technologies, Santa Clara, CA, USA) with an Agilent 2100 bioanalyzer (Agilent Technologies). Isolated RNA was hybridized to the Affymetrix GeneChip Mouse Gene 1.0 ST Array according to the manufacturer protocol (Thermo Fisher Scientific, Waltham, MA, USA). We used the Significance Analysis of Microarray (SAM) method to identify probe sets with target in

Table 1
Real-time RT-qPCR primers.

Gene	Primer sequence	Product (bp)	Length	Tm (°C)	GC%	Reference
<i>Comt1</i>	F: 5' TTGACGAGGGATGAGAG 3'	102	18	55	55.56	
	R: 5' GCAACAGGAGAACCAAATG 3'		18	55	55.56	
<i>Alox-8</i>	F: 5' AGCACAGAGATATGT 3'	245*	18	53	44.44	
	R: 5' CATTGAGGATGTTGGTGT 3'		19	54	44.37	
<i>Lpl</i>	F: 5' AGTTTCATTACCAAGCT 3'	231*	19	52	42.11	
	R: 5' CTGAAGTAGGAGTCCTTA 3'		19	53	47.37	
<i>Cfos</i>	F: 5' AAGTAGGAGCACTATCTC 3'	117	18	50	44.44	
	R: 5' CTGGAGTGATCTGTC 3'		18	50	44.44	
<i>Tnf "see"</i>	F: 5' AGGCACTCCCCAAAGATG 3'	123	20	60	55.00	Lambertsen et al., 2009
	R: 5' TCACCCCCAAGGCTCAGTAGACA 3'		24	63	50.00	
<i>Tnf "no see"</i>	F: 5' TCTTCTCATCTCTGCTGTGGC 3'	100	22	61	50.00	Lambertsen et al., 2009
	R: 5' AGGCCATTGGAAACTCTCATC 3'		23	61	47.83	
<i>Tnfrsf1</i>	F: 5' GCCCGAACTCATCCATCATTG 3'	91	24	61	50.00	Lambertsen et al., 2007
	R: 5' GGCTGGGAGGGCTGAGTTAG 3'		24	70	70.83	
<i>Tnfrsf2</i>	F: 5' GCCCAGCAAATCTCAAGCATC 3'	133*	21	64	57.14	Lambertsen et al., 2007
	R: 5' TCCTAACATCAGCAGACCACTG 3'		23	62	52.17	
<i>Il1b</i>	F: 5' TGTAAATGAAAGCACAC 3'	68*	20	56	45.00	Clausen et al., 2016
	R: 5' TCTTCTTGGGATATGCTTGG 3'		21	56	42.86	
<i>Il1a</i>	F: 5' GTGCCAAGAAAGATAAGATG 3'	78	21	56	42.86	Clausen et al., 2016
	R: 5' GTCTCTGTTTCACTGAA 3'		22	56	40.91	
<i>Il1rn</i>	F: 5' AACCAAGCTATTGCTGGTACTA 3'	95*	23	60	43.48	Clausen et al., 2016
	R: 5' GCCCAAGAACACACTATGAAAGTC 3'		24	62	50.00	
<i>Scl6a4 (5-HTT)</i>	F: 5' CTCTACTATAACACCTCA 3'	182	20	51	40.00	
	R: 5' CGAAGTAAACTCCATC 3'		18	50	44.44	
<i>Probe</i>	R: 5' CGCTCTACTACCTCATCTCTCT 3'		24	59	54.00	
	F: 5' CAGCAGAACAGAAATCAA 3'		19	51	36.84	
<i>Htr2a</i>	F: 5' GTGACTTAAAGCAGAAA 3'	187	20	51	35.00	
	R: 5' GTGAGTAAAGCAAA 3'		21	54	52.00	
<i>Probe</i>	F: 5' CGAGCAGCCAGGAACCTTCA 3'		21	54	35.00	
	R: 5' CGGAAGTAGTGAGAACCTGTT 3'	114	25	60	44.00	Lambertsen et al., 2009
<i>Itgam (CD11b)</i>	R: 5' CTIATAATCCAAGGATCACGAAATT 3'		27	60	37.04	
	F: 5' GTCCAGTAATCCACCTCA 3'		85	19	54	47.37
<i>Nnt</i>	F: 5' CACCAACGCTTCAAGTAG 3'		18	54	55.56	
	R: 5' GTCCAGTAATCCACCTCA 3'	76	18	60	55.60	
<i>Itpk1</i>	F: 5' GTGCTGAGGAGTCTATCT 3'		19	61	47.40	
	R: 5' CGTGCCTGCTTCAAGA 3'	330*	19	58	52.63	
<i>Tacr3</i>	R: 5' GGTAGACCTGCTGGATATT 3'		22	58	45.45	
	F: 5' TGAGGGAGCTGGGAATATAG 3'	206*	21	58	52.38	
<i>Snca</i>	R: 5' CTAGAGGAGTGGTCAATGA 3'		22	58	45.45	
	F: 5' GTCCAGTAAACCACTACAA 3'	240*	22	58	45.45	
<i>Park2</i>	R: 5' TTGGGTGTGCTCACATT 3'		20	57	45.00	
	F: 5' CCCATGAAACATCCACCT 3'	276	24	58	45.83	
<i>Asic</i>	R: 5' CCCATGAAACATCCACCT 3'		20	57	50.00	
	F: 5' AAATCAACAAAGCTGCTGTA 3'	93*	21	59	47.62	Meldgaard et al., 2006
<i>Hprt1</i>	R: 5' AAATCAACAAAGCTGCTGTA 3'		24	61	41.67	

F, forward; R, reverse.

Red demarcates exon-exon junction.

*One or more exon-exon junction(s) within the PCR product.

transcripts that were significantly differentially expressed between WT and TNF^{-/-} mice (Tusher et al., 2001). SAM analysis was performed using MultiExperimentViewer Software v. 4.5.1. (Dana-Farber Cancer Institute, Boston, MA, USA), 70 unique permutations and an s0 value selected by Tusher's method (Saeed et al., 2006; Saeed et al., 2003; Tusher et al., 2001). A false discovery rate (FDR) < 5% was considered evidence of statistical significance. Significant genes were analyzed for Gene Ontology (GO) terms and Kyoto Encyclopaedia of Genes and Genomes (KEGG) pathways related to neurogenesis and inflammation in <http://pantherdb.org> (version 13.1), string-db.org (version 10.5), and <http://www.genome.jp/>. Primary microarray data were submitted to the public database at the GEO website (<http://www.ncbi.nlm.nih.gov/geo>; record number: GSE134178).

2.6. Real-time RT-qPCR

Real-time RT-qPCR was performed for Catechol-O-methyl transferase (*Comt1*), Arachidonate 8-lipoxygenase (*Alox-8*), Lipoprotein lipase (*Lpl*), c-Fos (*Cfos*), TNF (*Tnf*), TNFR1 (*Tnfrsf1a*), TNFR2 (*Tnfrsf1b*), IL-1 β (*il1b*), IL-1 α (*il1a*), IL-1 receptor antagonist (*IL-1Ra*, *Il1rn*), 5-Hydroxy tryptamine transporter (5-HTT, *Scl6a4*), 5-Hydroxytryptamine receptor 2A (*Htr2a*), CD11b (*Itgam*), Nicotinamide nucleotide transhydrogenase (*Nht*), Inositol-trisphosphate 3-kinase A (*Itpka*), Tachykinin receptor 3 (*Tacr3*), Synuclein alpha (*Snca*), Parkin RBR E3 Ubiquitin Protein Ligase (*Park2*), and Acid-sensing ion channel 1 (*ASIC1*) using cDNA isolated from brain tissue from 2-month old WT and TNF^{-/-} male mice on an iCycler (Bio-Rad Laboratories, Hercules, CA, USA) as

previously described (Clausen et al., 2014; Clausen et al., 2008; Clausen et al., 2016; Lambertsen et al., 2007) with primer sequences found in Table 1. For *Tnf*, we used both no-see and see primers. The no-see primer set was designed to target the *Tnf* gene flanking the inserted neomycin cassette and thus should not detect *Tnf* mRNA. The see *Tnf* primers were designed to target outside the neomycin cassette, resulting in expression of a non-functional *Tnf* mRNA (Lambertsen et al., 2009; Pasparakis et al., 1996). Values were normalized to hypoxanthine phosphoribosyltransferase 1 (*Hprt1*) as the reference gene and calibrated to a pool of unmanipulated C57BL/6 mice (Lambertsen et al., 2009). Primers were designed to target exon-exon junctions whenever possible and were purchased from TAG Copenhagen (Copenhagen, Denmark). All samples were analyzed using SYBR green except for *Htr2a* and *Slc6a4* that were analyzed using TaqMan probes. Transcript levels within two-fold threshold of methodological resolution were not subjected to statistical analysis (Meldgaard et al., 2006).

2.7. Western blotting

Brain tissue (one hemisphere) from 4-month old WT, TNF^{-/-}, and C57BL/6 mice treated with saline, XPro1595, or etanercept were lysed with complete mesoscale lysis buffer (Mesoscale Discovery), sonicated, and centrifuged for 20 min at 14,000g, 4 °C. Supernatants were collected and stored at -80 °C. Protein concentrations were determined using Micro BCA™ protein assay kit (Thermo Fisher Scientific) according to the manufacturer's instructions. Protein samples (10 µg) were separated on SDS-PAGE 4–12% Bis-Tris- gels (Thermo Fisher

Table 2
Antibodies applied for immunohistochemical staining and Western blotting.

Protein of interest	Antibody	Isotype	Species of origin	Cat. #
IMMUNOHISTOCHEMISTRY				
<i>Primary antibodies:</i>				
<i>E13.5:</i>				
Phosphohistone H3 (Ser10)	PH3 (1:500)	Ig fraction	Rabbit	06-570, Sigma-Aldrich
Ionized calcium binding adaptor molecule 1	Iba1 (1:500)	Ig fraction	Goat	ab5076, Abcam
Doublecortin	DCX (1:500)	Ig fraction	Rabbit	ab18723, Abcam
Claudin-5	CLDN5 (1:500)	Ig fraction	Rabbit	LC-C402200, Nordic Biosite
Glucose transporter-1	GLUT-1 (1:500)	Ig fraction	Rabbit	ab652, Abcam
Albumin	Albumin (1:500)	Ig fraction	Goat	ab19194, Abcam
<i>P7:</i>				
Ionized calcium binding adaptor molecule 1	Iba1 (1:500)	Ig fraction	Rabbit	019-19741, Wako Chemicals
Ki-67	Ki-67 (clone SP6) (1:500)	IgG	Rabbit	MA5-14520, Thermo Scientific
<i>Adult:</i>				
Integrin alpha M chain (CD11b)	CD11b (clone 5C6) (1:600)	IgG2b	Rat	MCA711, Bio-Rad
Ionized calcium binding adaptor molecule 1	Iba1 (1:350)	Ig fraction	Rabbit	ab5076, Abcam
5-Bromodeoxyuridine	BrdU (clone BU1/75 (ICR1)) 1:600	IgG2a	Rat	MCA2060GA, Bio-Rad
<i>Isotype/serum controls:</i>				
Un-conjugated		IgG2b	Rat	IG-851125, Nordic Biosite
Un-conjugated		Ig fraction	Rabbit	X0903, DakoCytomation
Un-conjugated		IgG2a	Rat	P54605M, Nordic Biosite
<i>Secondary antibodies:</i>				
Anti-rabbit IgG	Biotinylated (1:100)	Ig fraction	Goat	BA-1000, Vector Labs
Anti-rabbit IgG	Envision + HRP (1:200)	Ig fraction	Goat	K400311-2, Agilent
Anti-goat IgG	Biotinylated (1:100)	Ig fraction	Horse	BA-9500, Vector Labs
Anti-rat IgG	Biotinylated (1:200)	Ig fraction	Goat	BA-9400, Vector Labs
Anti-rat IgG	Biotinylated (1:100)	Ig fraction	Goat	BA-9400, Vector Labs
<i>Tertiary antibodies:</i>				
Vectastain ABC HRP kit	ABC (Avidin/Biotin)			PK-4000, Vector Labs
Streptavidin	HRP-conjugated streptavidin (1:200)			RPN1231, GE Life Sciences
WESTERN BLOTTING				
<i>Primary antibodies:</i>				
Collagen Triple Helix Repeat Containing 1	CTHRC1 (1:800)	Ig fraction	Rabbit	ab85739, Abcam
Frizzled-6	FZD6 (1:1,000)	Ig fraction	Rabbit	ab229663, Abcam
Actin	Actin (clone C4) (1:100,000)	IgG1	Mouse	MAB1501, Merck Life Science
<i>Secondary antibodies:</i>				
Anti-rabbit IgG	HRP-conjugated (1:2,000)	Ig fraction	Goat	P044801-2, Agilent
Anti-mouse IgG	HRP-conjugated (1:2,000)	Ig fraction	Goat	P044701-2, Agilent

Scientific) and wet transferred to an Immobilon-P transfer membrane (Merck Life Science, Darmstadt, Germany). The membrane was blocked using 5% non-fat milk in 0.05 M tris-buffered saline + 0.05% Tween-20 (TBST, Sigma-Aldrich). Anti-CTHRC1 antibody or anti-FZD6 antibody (Table 2) was added for overnight incubation at 4 °C. Anti-actin antibody (Table 2) was used as a loading control. The next day, secondary horse-radish peroxidase (HRP)-conjugated anti-rabbit IgG or anti-mouse IgG (Table 2) was added. Membranes were developed using SuperSignal™ West Dura Extended Duration Substrate (Thermo Fisher Scientific) and ChemiDoc™ MP Imaging System (Bio-Rad). Analysis was performed on un-manipulated images by measuring the intensity of the Western blotting bands using Image Lab™ software (Bio-Rad) according to the manufacturer's instructions. The mean sample intensity of the band of interest was divided by the corresponding mean loading control intensity for normalization and presented as relative intensity to WT for the TNF^{-/-} mice, or relative intensity to saline for XPro1595- and etanercept-treated mice.

2.8. High-performance liquid chromatography of brain monoamines

Brains from 2-months-old male WT and TNF^{-/-} mice were dissected into ipsi- and contra-lateral sides of frontal cortex, occipital cortex, striatum, hippocampus, thalamus + hypothalamus, and cerebellum and kept on dry ice. Dissected tissue was briefly sonicated in Eppendorf tubes containing 200–1,000 µL (1:20 weight/volume) of ice-cold 0.1 M perchloric acid (PCA) (Sigma-Aldrich) containing anti-oxidants (Na₂S₂O₅ and Na₂-EDTA, Sigma-Aldrich) and centrifuged at 20,627 × g for 20 min at 4 °C. The supernatant was used for reverse-phase high-performance liquid chromatography (HPLC) analysis. Levels of noradrenalin (NA), dopamine (DA), serotonin (5-hydroxytryptamine, 5-HT), the DA metabolites 3,4-dihydroxyphenylacetic acid (DOPAC) and homovanillic acid (HVA), and the 5-HT metabolite 5-hydroxyindoleacetic acid (5-HIAA) were assessed by HPLC with electrochemical detection, essentially as previously described (Gramsbergen et al., 2002) but using a mobile phase consisting of 10% methanol (volume/volume) (Sigma-Aldrich), citric acid monohydrate (Sigma-Aldrich), octane-1-sulfonic acid sodium salt (Sigma-Aldrich), and EDTA (Sigma-Aldrich) dissolved in Milli-Q water and pH adjusted to 4.0 (Santiago et al., 2010). The Merck-Hitachi HPLC system consisted of an L-7100 pump, an L-7200 autosampler, a D-7000 interface, and an electrochemical detector with inbuilt column oven (Antec Leyden – DECADE, Zoeterwoude, Netherlands), connected to a computer equipped with D-7000 version 2.0 chromatography software. The mobile phase was pumped at a flow rate of 0.9 ml/min through a Waters Spherisorb S5 ODS2 guard column (4.6 × 30 mm) and a Waters Spherisorb S3 ODS2 cartridge analytical column (4.6 × 150 mm, Waters, Milford, MA, USA). A single amount of 20 or 10 µL of external standards (0.5 or 0.25 pmols) per compound was injected and peak heights were used to calculate the absolute amounts of the compounds of interest in the brain tissue samples. Calibration curves were based on peak height at 0.5 or 0.25 pmol and 0 pmol (injection with no compound gives no peak, thus calibration curve is forced through zero). Peak heights were linearly related to the amounts on the column, thereby allowing calculations on the basis of a single amount of external standard for a particular compound. Brain tissue samples were diluted appropriately, so that peaks of the compounds of interest were within the detectable range. To allow calculation of all compounds of interest, different dilutions and multiple injections were necessary.

2.9. Histology

Tissue sections from E13.5 fetuses and P7 mice were heated at 60 °C for 1 h, cleared in xylene (VWR, Søborg, Denmark) (2 × 5 min), rehydrated in ethanol (2 × 3 min in 99%, 1 × 3 min in 96%, and 1 × 3 min in 70%), and then rinsed in running tap water followed by distilled water (dH₂O). For hematoxylin and eosin (HE) staining, sections were

placed in filtered Mayer's hematoxylin (Sigma-Aldrich) for 3 min, rinsed 3 × in dH₂O, and placed in running tap water for 10 min. Next, sections were rinsed in dH₂O and placed in 0.2% eosin mixed 1:5 with 70% ethanol for 2 min. Sections were dehydrated in ethanol, cleared in xylene, mounted, and coverslipped using Depex mounting media (VWR). For Toluidine blue (TB) (Sigma-Aldrich) staining, sections were placed in 70% ethanol overnight at room temperature. The next day, sections were rinsed 10 × in dH₂O, placed in TB solution for 3 min, rinsed 10 × in dH₂O, and cleared in 96% and 99% ethanol followed by xylene. Sections were coverslipped using Depex mounting media.

2.10. Immunohistochemistry

One series of sections from E13.5 and P7 mice was deparaffinated and, together with one series of tissue sections from 2-months old WT and TNF^{-/-} and from mice treated with saline, XPro1595 or etanercept, was blocked for endogenous peroxidase activity in either 0.2%, 3%, or 5% H₂O₂ in methanol, depending on the optimized staining protocol, for 30 min to 1 h followed by incubation in primary antibodies overnight at 4 °C. All primary and secondary antibodies used for immunohistochemistry are listed in Table 2 along with tertiary reagents and isotype and serum controls. For identification of EdU⁺ cells, sections were stained with Click-it™ EdU Alexa Fluor™ 488 Imaging Kit (Thermo Fisher Scientific) according to the kit protocol. Isotype controls and IgG controls for polyclonal rabbit antibodies were done using comparable IgG concentrations. In addition, omission of primary antibodies was used as negative controls. Sections were developed in 3,3'-diaminobenzidine (DAB) (Sigma-Aldrich) and mounted as previously described (Lambertsen et al., 2011).

2.11. Cell estimate

E13.5: We selected sections at the level of the interventricular foramina (Bregma –0.4 in the adult brain), corresponding to the putative somatosensory cortex. The number of proliferating cells was estimated by manually counting PH3⁺ cells on a Leica DMR200 microscope in the ventricular zone (VZ) and subventricular zone (SVZ). The VZ was defined as the layer of cells immediately adjacent to the ventricles, while the SVZ formed a defined band between the VZ and the edge of the cortex. To exclude variation in VZ length due to natural size variation as a source of error, the VZ length was measured in ImageJ (NIH) using the "freehand line" tool following recommendations of the ImageJ developers (Schneider et al., 2012). PH3 cell counts along the VZ surface were normalized to the length of the VZ in the dorsal cortex for each section examined resulting in a value for the number of cells/pixel. The number of Iba1⁺ microglia was counted manually with a clicker in the developing neocortex in three sections per animal placed immediately adjacent to those where analysis of PH3⁺ proliferating cells was carried out. Two measurements were made: the total number of microglia in the brain and the percentage of non-rounded microglia (i.e. ramified defined as cells with more than 2 lines of asymmetry). Spherical Iba1⁺ cells in close proximity to vasculature or red blood cells were assumed to be blood monocytes and were excluded from the count.

P7 and adult mice: The total number of cells was estimated using a BX50 microscope (Olympus, Ballerup, Denmark) coupled to the computer-assisted newCAST stereology system from Visiopharm (Hørsholm, Denmark). Cells were counted using a 100 × oil lens and a counting frame of 799.8 µm², with step size of 400 µm (microglia and neurons) and 200 µm (Ki67⁺ cells) (Lyck et al., 2007). The total number of cells was calculated using the formula: $N = \Sigma Q^- \times (1/tsf) \times (1/asf) \times (1/ssf)$, where ΣQ^- represents the total number of counted cells, tsf the thickness sampling fraction ($tsf = t/h = 15.5 \mu m/8 \mu m$ for P7 and $20 \mu m/12 \mu m$ for adult mice), asf the area sampling fraction ($a/frame)/a(step) = 799.8 \mu m^2/160,000 \mu m^2$ in neocortex or $799.8 \mu m^2/40,000 \mu m^2$ in dentate gyrus), and ssf the sections sampling fraction

(ssf = 1/6). The total number of Iba1⁺ microglia, CD11b⁺ microglia, and TB⁺ neurons was estimated in the right hemisphere of the neocortex, while the number of Ki67⁺ proliferating cells was estimated in the dentate gyrus of the hippocampus. Estimated cell numbers were multiplied by two for P7 mice in order to take cell numbers in the contralateral side of the brain into account. Identification of neurons in the TB staining was based on the typical neuronal morphology of large cell bodies, pale nucleus containing one nucleolus, and cytoplasm containing Nissl substance (Lyck et al., 2007).

In the hippocampus, the total number of BrdU⁺ and EdU⁺ cells throughout the granular cell layer of the dentate gyrus of mice treated with saline, XPro1595, or etanercept were counted manually using a 20× objective. Cells lying more than 20 µm deep into the hilum were not included. All cell estimates were made with the observer blinded to the genotype.

2.12. Volume calculations and cell density

Photomicrographs were acquired using the 4× (E13.5) or 2× (P7) lens and 1.25 tube factor on an Olympus BX51 microscope fitted with an Olympus D973 camera and coupled to CellSens Software (Olympus). Light settings were kept constant for all pictures taken. Densitometry was performed in the developing neocortex from images of E13.5 tissue stained for albumin, claudin-5, and glucose transporter 1 (GLUT1) using Image J analysis software (NIH) as per directions of the Image J developers (<http://rsb.info.nih.gov/ij>). Briefly, all TIFF files were gray-scaled (8 bits) using Adobe Photoshop CS5 for Mac, pictures imported into Image J and background subtracted. Each section was delineated using the “freehand tool” based on microscopic landmarks (Schambra et al., 1991) and the densitometry measured across each section was estimated using the Log10(Mean value/255) calculation. A mean density was found for each section and presented as relative density to WT. The length and area of the ganglionic eminence (GE) were estimated in HE-stained sections from E13.5 fetuses. The volumes of the ventricles, subependymal zone (SEZ), and cortex (bregma 1.70 to −0.82) were estimated in HE-stained sections from P7 mice and the density of ki67⁺ cells was estimated in the SEZ, as described above. The neocortex was delineated as previously described (Lyck et al., 2007) and contained the anterior part of the agranular insular cortex, orbital cortex, cingulate cortex, frontal cortex, pre-limbic cortex, granular insular cortex, retrosplenial agranular cortex, anterior parts of retrosplenial granular cortex, entorhinal cortex, parietal cortex, temporal cortex, and all areas of the occipital cortex. Cortex volume was estimated using the principle of Cavalieri (Gundersen et al., 1988). Volumes of lateral ventricles, SEZ, and cortex in P7 mice were multiplied by 2 in order to take the contralateral hemisphere into account.

2.13. Behavioral tests

The behavioral battery incorporated several different types of tests conducted in the following order: (1) Y maze test, (2) Open field test, (3) Elevated plus maze test, and (4) Barnes maze test. Mice were given a least one day off between tests, which were conducted in order of least to most stressful to minimize effects of previous testing. All behavioral tests were performed with the observer blinded to the genotype or treatment.

Y maze. The Y maze was used to evaluate short-term memory and exploratory behavior in 4-month old WT and TNF^{−/−} mice, and in C57BL/6 mice before (at 2 months of age) and after treatment (at 4 months of age) with TNF inhibitors as previously described (Lambertsen et al., 2012). In brief, each mouse was placed in the arm designated (A) of the Y-maze field. Except for the first two, the number of entries into each arm (A, B, C) was recorded manually over an 8 min period and spontaneous alternation calculated based on these numbers.

Open field. The open field test was performed one and two months after the start of TNF inhibitor treatment to test anxiety and locomotor

activity in C57BL/6 mice as previously described (Lambertsen et al., 2012). The open field test was performed using a non-transparent plastic square arena measuring 45 (W) × 45 (D) × 40 (H) cm. The arena was divided into three zones (wall, intermediate and center), and spontaneous movements in each zone were tracked using the SMART 3.0 Video Tracking System (Panlab Harvard Apparatus, Barcelona, Spain) connected to a high-resolution color video camera (SSC-DC378P, Biosite, Stockholm, Sweden). Mouse behavior was recorded over a 10 min period and total distance travelled (m), as well as time spent in each zone were automatically recorded. A center/perimeter ratio was calculated as previously described (Lambertsen et al., 2012). Rearing, as a measure of stereotypical mouse behavior, was manually recorded and expressed as total number of events.

Elevated plus maze. The elevated plus maze was used to assess anxiety-related behavior in 4-months old WT and TNF^{−/−} as previously described (Ellman et al., 2017). The elevated plus maze apparatus consisted of two open arms and two closed arms (30 cm × 5 cm). Each mouse was placed in the center of the maze with the head facing towards the open arm. During a 5 min test, the total distance travelled and the time spent in the closed and open arms were recorded using the SMART video tracking software (Panlab). A open/closed arm ratio was calculated based on the times spent in each arm as a measure of anxiety-related behavior.

Barnes maze. After 7 weeks of saline, XPro1595, or etanercept treatment, C57BL/6 mice and 4-months-old WT and TNF^{−/−} mice were subjected to Barnes maze for assessment of long-term memory and spatial recognition. The test was performed according to the protocol previously described (Ellman et al., 2017). Mice interacted with the Barnes maze in three phases: habituation (1 day), training (3 days), and probe (1 day). They were housed in the behavior room during the whole experiment. On the habituation day, mice were placed in the center of the maze inside a transparent starting cylinder (diameter: 8 cm; height: 12.5 cm) for 30 s. Then mice were guided slowly by moving the cylinder towards the target hole that lead to the escape box while loud heavy metal music was played. After 10–15 s, the cylinder was removed and mice were given 3 min to independently enter through the target hole into the escape box. If they did not enter on their own during that time, they were gently guided. Mice were allowed to stay in the escape box for 1 min with the music turned off before being returned to a holding cage. In the training phase, mice were placed inside a non-transparent starting cylinder placed in the center of the maze for 15 s. At the end of the holding period, the music was started and they were allowed to explore the maze for 3 min. If a mouse found the escape box and entered it during that time, it was allowed to stay there for 1 min. If it did not find the escape box, it was gently guided towards it. Each mouse was provided a 20–30 min inter-trial resting period. The total number of trials each day was 5. On the probe day, the escape box was removed and the mice were placed inside the starting cylinder placed in the center of the maze for 15 s, the music was turned on, and the cylinder removed. Each mouse was given 2 min to explore the maze, whereafter the mouse was returned to its cage. After the first 4 trials, external cues were exchanged 180° and the test was repeated, in order to test whether the mouse used external clues to navigate after. Measures of time spent in the quadrant where the escape box used to be (target quadrant) were recorded, along with time spent in the positive, negative and opposite quadrants. For these analyses, the maze was divided into quadrants of 5 holes.

2.14. Phagocytosis assay

In order to test the effect of TNF on microglial phagocytic activity, primary microglia derived from P0-P2 days old C57BL/6 mice were plated, activated and incubated with fluorescent beads essentially as previously described (Al-Ali et al., 2017; Yli-Karjanmaa et al., 2019). As a measure of phagocytic activity, the number of engulfed beads/cell and cell morphology measured as cell area, membrane irregularity and

perimeter length were estimated by the automated counting software Puntomorph (<https://github.com/HA-Lab/PuntoMorph>) (Al-Ali et al., 2017). In order to ensure correct data processing, data were automatically transformed into excel data using an in-house made python

program PuntoCalc.

For purification of primary microglia, brains were collected in ice-cold Hanks' Balanced Salt Solution (HBSS) without Ca^{2+} and Mg^{2+} (Thermo Fisher Scientific), cortices dissected and processed using

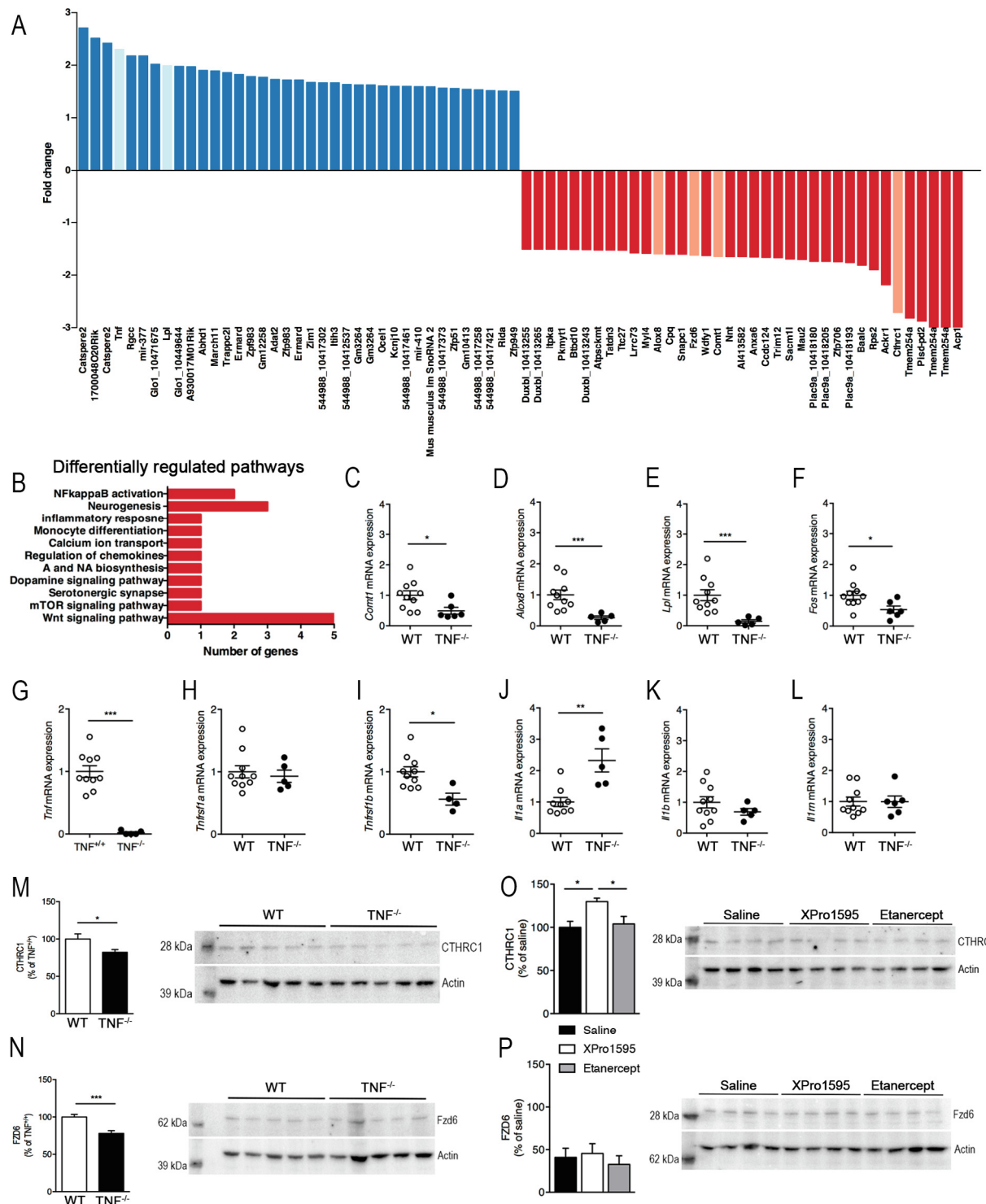


Fig. 1. TNF deficiency alters expression of genes and proteins in WNT signaling pathway. (A) RNA fold change of the differently expressed genes in $\text{TNF}^{-/-}$ ($n = 4$) versus WT ($n = 4$) brains. Blue is upregulated and red is downregulated in $\text{TNF}^{-/-}$ mice compared with WT mice. Bars in lighter colors represent genes verified using RT-qPCR. (B) Pathway analysis of differentially regulated genes. (C-F) *Comt1* (C), *Alox-8* (D), *Lpl* (E), and *Fos* (F) mRNA downregulation in $\text{TNF}^{-/-}$ mice (4–10/group). (G-L) Gene expression of *Tnf* (G), *Tnfrsf1a* (H), *Tnfrsf1b* (I), *Il1a* (J), *Il1b* (K), *Il1rn* (L) (4–10 mice/group). (M-N) CTHRC1 (M) and FZD6 (N) protein levels were reduced in $\text{TNF}^{-/-}$ mice compared to WT mice (12–13/group). (O) CTHRC1 protein levels were upregulated in XPro1595-treated mice compared to saline- and etanercept-treated mice (7/group). (P) FZD6 protein levels were comparable in saline-, XPro1595-, and etanercept-treated mice (5/group). * $p \leq 0.05$, ** $p < 0.01$, *** $p < 0.001$, Student's t-test or one-way ANOVA with Tukey's post hoc. (For interpretation of the references to color in this figure legend, the reader is referred to the web version of this article.)

Neural Tissue Dissociation Kit (P) (Miltenyi Biotech, Lund, Sweden) according to the manufacturer's protocol. Next, microglia were purified by MACS sorting using magnetic CD11b⁺ beads on LS columns (Miltenyi Biotech) and cultured as 80,000–100,000 cells/well in 20% pre-warmed foetal bovine serum (FBS)-DMEM complete medium (76%

Dulbecco's Modified Eagle Medium (DMEM) + 20% heat inactivated FBS), 1% non-essential amino acids, 1% penicillin streptomycin, 1% GlutaMax and 1% pyruvate (all from Thermo Fisher Scientific) on poly-L-Lysine-coated plates in a humified CO₂ incubator at 37 °C. After 2–3 days, half of the media was changed to culture medium B (86%

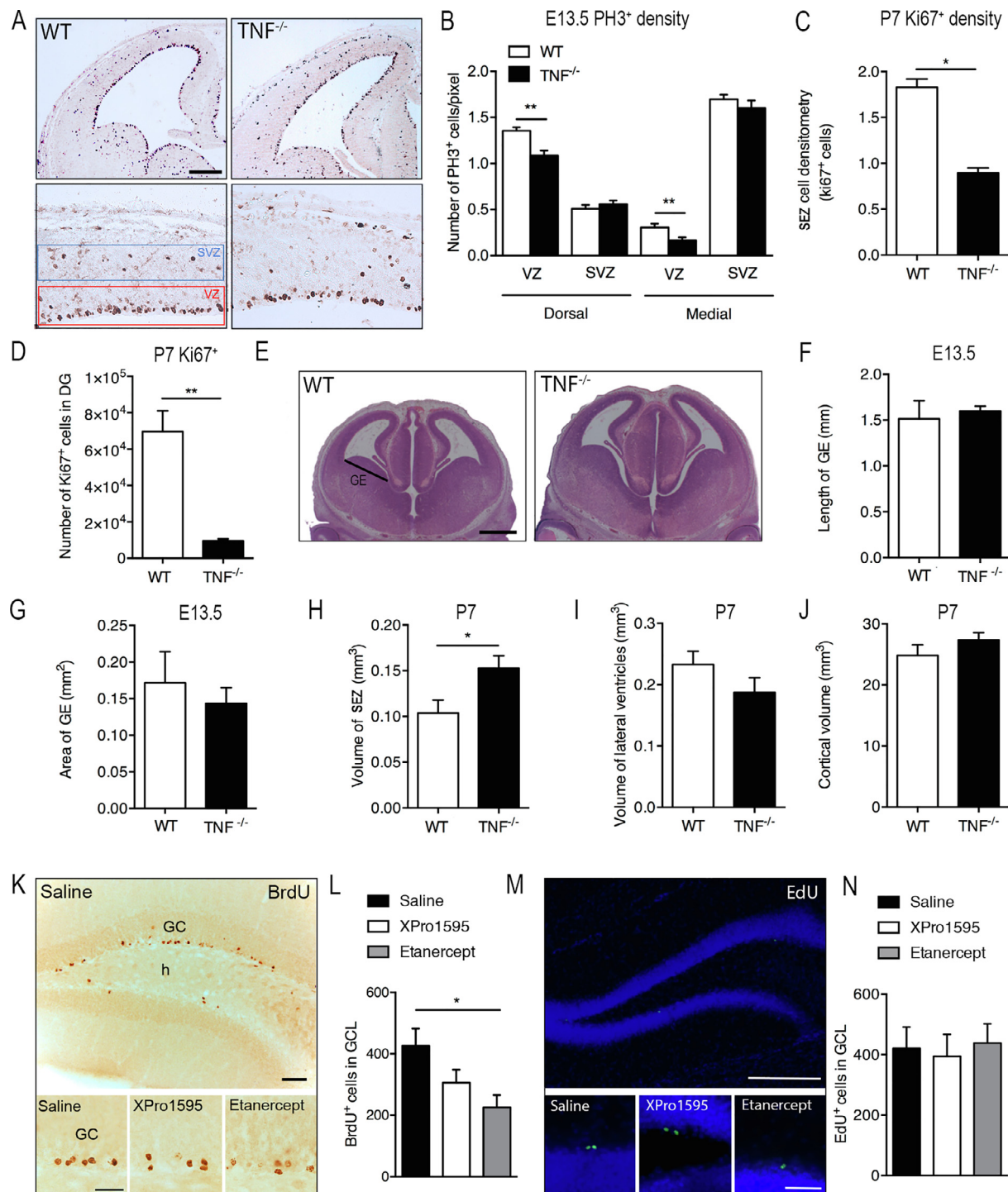


Fig. 2. TNF deficiency decreases neurogenesis. (A) PH3⁺ cells in SVZ and VZ in E13.5 WT and TNF^{-/-} mice. Scalebar = 200 μm. (B) Estimation of PH3⁺ cells/pixel in SVZ and VZ in E13.5 mice (8–12/group). (C) SEZ Ki67 cell density and (D) number of Ki67⁺ cells in the dentate gyrus (DG) of P7 WT and TNF^{-/-} mice (4–6/group). (E) HE-stained E13.5 brains used for GE length and area estimations. Scalebar = 200 μm. (F) GE length in E13.5 mice (3–10/group). (G) GE area in E13.5 mice (3–10/group). (H) SEZ volume in P7 mice (6–7/group). (I) Volume of lateral ventricles in P7 mice (6–7/group). (J) Cortical volume in P7 mice (6–7/group). (K) BrdU⁺ cells in granular cell layer (GC) of dentate gyrus in saline-, XPro1595-, and etanercept-treated mice. Scalebars = 100 μm and 10 μm (high magnification). (L) Number of BrdU⁺ cells in granular cell layer (GCL) of dentate gyrus in saline-, XPro1595-, and etanercept-treated mice (5–8/group). (M) EdU⁺ cells in dentate gyrus of saline-, XPro1595- and etanercept-treated mice. Scalebars = 100 μm and 10 μm (high magnification). (N) Number of EdU⁺ cells in granular cell layer (GCL) of dentate gyrus in saline-, XPro1595-, and etanercept-treated mice (6–7/group). *p ≤ 0.05, **p < 0.01, Student's t-test or one-way ANOVA with Tukey's post hoc.

DMEM, 10% FBS, 1% MEM, 1% penicillin streptomycin, 1% GlutamaxTM, 1% pyruvate). Four days after the media change microglia were activated by adding 100 ng/mL lipopolysaccharide (LPS) (Invitrogen, Thermo Fisher Scientific) and treated with either 100 or 200 ng/mL XPro1595, or 100 or 200 ng/mL etanercept. Non-stimulated cells and cells stimulated with LPS were kept as controls. Microglia were then incubated at 37 °C for 24 h. Next day, FluoSpheresTM Carboxylate-Modified Microspheres (1.0 mm, 505/515, yellow/green fluorescent) (Thermo Fisher Scientific) were added onto the cultured cells. After 2 h, phagocytosis was terminated by adding ice-cold DMEM for 2–5 min. Cells were fixed with 4% PFA, blocked in 5% normal goat serum in TBS and incubated overnight in anti-Iba1 antibody (1:500, Table 2). The next day, cells were stained using alexa 594-conjugated anti-rabbit antibody (1:750, Molecular Probes) and 4',6-diamidino-2-phenylindol (DAPI) (Thermo Fisher Scientific) and mounted using ProLong Diamond. In total, 12–15 pictures were randomly taken from each coverslip using a 20× magnification with an Olympus Fluoview 1000 confocal microscope to ensure that it was possible to analyze at least 9 pictures per coverslip. Two independent experiments were performed.

2.15. Statistics

Statistical comparisons used two-tailed Student's unpaired *t*-test for RT-qPCR, Western blot, monoamines, number of proliferating cells and neurons, the morphological analysis of E13.5 and P7, albumin, GLUT1 and claudin-5 expression, body weight, Y maze test, and elevated plus maze test. Comparisons between the number of microglia in E13.5, P7, adult WT and TNF^{−/−} mice used one-tailed Student's *t*-test as we previously found TNF^{−/−} mice to have significantly fewer microglia than WT (Lambertsen et al., 2009). Comparisons between the mice treated with saline, XPro1595, or etanercept used i) one-way ANOVA followed by Tukey's multiple comparisons test for Western blot, multiplex ELISA, proliferating cells, number of microglia, and Y maze test, ii) Repeated measures two-way ANOVA followed by Tukey's *post hoc* test for body weight, and iii) Student's paired *t*-test to compare performance in the open field test at one and two months after treatment. Phagocytosis assay was analysed using one-way ANOVA followed by Tukey's *post hoc* test. Barnes maze learning curves from day 1 to day 4 were analyzed by repeated measures two-way ANOVA followed by Tukey's *post hoc* test. Comparisons of the average latency time in Barnes maze between WT and TNF^{−/−} mice used Student's unpaired *t*-test, and comparisons between saline-, XPro1595-, or etanercept-treated mice by one-way ANOVA followed by Tukey's *post hoc* test. The spatial memory retention on day 5 of Barnes maze was tested by repeated measures two-way ANOVA followed by Sidak's multiple comparison's test. Data are presented as mean ± SEM. Statistical significance was set at $p \leq 0.05$.

3. Results

3.1. TNF deficiency alters the expression of genes related to neurogenesis and WNT signaling

To study cellular changes resulting from developmental TNF deficiency, we assessed the gene expression profile in the whole brain by whole-transcript microarray analysis of 28,853 genes in 2-months old TNF^{−/−} versus WT mice. We found 66 differentially expressed genes to be either upregulated (Fig. 1A, blue bars) or downregulated (Fig. 1A, red bars) in TNF^{−/−} compared to WT mice, which included genes related to proinflammatory mechanisms, neurotransmission, lipid metabolism, and WNT signaling. By KEGG pathway analysis we identified the WNT and nuclear factor-kappa B (NF-κB) signaling pathways, as well as neurogenesis and monoamine pathways related genes as the most affected (Fig. 1B). Select differentially expressed genes (Fig. 1A, bars indicated by light blue and light red colors) found through gene

chip analysis were verified by RT-qPCR (Fig. 1C-G). *Comt1*, *Alox-8*, and *Fos* were significantly lower in adult TNF^{−/−} mice (Fig. 1C-F). On the microarray, *Tnf* was significantly upregulated, evidenced by the “*Tnf see*” primers (Supplementary table 1). However, as this is a non-functional *Tnf* mRNA, we also measured expression of functional *Tnf* mRNA using the “*Tnf no-see*” primers. Expression of intact *Tnf* was disrupted in TNF^{−/−} mice, as expected (Fig. 1G). Expression of *Tnfrsf1a* was comparable between groups (Fig. 1H), and *Tnfrsf1b* was downregulated in TNF^{−/−} mice (Fig. 1I). Expression of IL-1 often correlates with TNF expression (Dinarello et al., 1986; Philip and Epstein, 1986), and we found that *Il1a* was upregulated in TNF^{−/−} mice (Fig. 1J), whereas *Il1b* and *Il1m* were comparable between groups (Fig. 1K,L). Finally, we also checked a number of genes involved in serotonergic and dopaminergic signaling, however, we saw no significant differences in expression of *Scl6a4*, *Htr2a*, *Itgam*, *Nnt*, *Itpk1*, *Tacr3*, *Snc1*, *Asic1*, and *Park2* mRNAs (Supplementary table 1).

Genes related to neurogenesis were also differentially expressed in TNF^{−/−} mice (Fig. 1A-B). Gene chip analysis showed *Cthrc1* and *Fzd6* expression to be significantly lower in TNF^{−/−} than WT mice (Fig. 1A). Western blotting verified that protein expression of CTHRC1 (Fig. 1M) and FZD6 (Fig. 1N) was lower in TNF^{−/−} mice compared to WT mice. In contrast, two months of XPro1595 treatment led to upregulation of CTHRC1 expression compared to saline and etanercept treatment (Fig. 1O). Pharmacological TNF inhibition did not affect expression of FZD6 (Fig. 1P).

3.2. TNF deficiency decreases cell proliferation

Due to the role of WNT signaling in cell proliferation, the observed altered RNA levels of genes in the WNT signaling pathway (Fig. 1A,B), and changes in levels of WNT-signaling-related proteins, CTHRC1 and FZD6 (Fig. 1M-N), we further investigated whether TNF deficiency might impact the number of proliferating cells in the developing brain. We analyzed the density of PH3⁺ proliferating cells in the developing neocortex of E13.5 mice (Fig. 2A-B) and the density and number of Ki67⁺ proliferating cells in P7 mice (Fig. 2C-D), comparing TNF^{−/−} mice to WT littermates. The number of PH3⁺ cells/pixel in the VZ was lower at E13.5 in TNF^{−/−} mice but was unchanged in the SVZ (Fig. 2B). The density of Ki67⁺ cells in the SEZ (Fig. 2C) and the total number of Ki67⁺ cells in the dentate gyrus (Fig. 2D) were significantly lower at P7 in TNF^{−/−} compared with WT mice.

To estimate potential changes in neurogenic zones, we also measured GE length and area in HE-stained sections from E13.5 mice (Fig. 2E-G) and estimated the volume of SEZ, lateral ventricles, and cortex in HE-stained sections from P7 mice (Fig. 2H-J). We observed no significant differences in GE length and area between TNF^{−/−} and WT mice at E13.5 (Fig. 2F-G). In P7 mice, SEZ volume was significantly larger in TNF^{−/−} than in WT (Fig. 2H), whereas the volumes of the lateral ventricles (Fig. 2I) and the neocortex (Fig. 2J) were comparable.

Due to the altered cell proliferation in the neurogenic zones of E13.5 and P7 mice, we investigated if long-term use of TNF inhibitors would cause similar changes in adult mice. First, we injected mice with BrdU (Fig. 2K-L) prior to treatment with saline, XPro1595, or etanercept to test the effect of long-term TNF inhibition on the number of BrdU⁺ cells in the dentate gyrus. Second, to test the effect of treatment on spatial learning and memory, we injected EdU (Fig. 2M-N) after 7 weeks of saline, XPro1595, or etanercept administration, just prior to subjecting the mice to a spatial leaning and memory test and 1 week before euthanasia. Etanercept treatment reduced the number of BrdU⁺ cells in the granular cell layer of dentate gyrus in adult mice compared to the saline-treated group, whereas XPro1595 had no effect (Fig. 2L). There were no differences in the number of EdU⁺ cells between groups (Fig. 2N).

3.3. TNF deficiency decreases the number of cortical microglia during development and increases the number of neurons in adult mice

Since absence of TNF during development decreased the number of proliferating cells and altered the spatial organization of the neurogenic zones of the brain, we assessed whether this was associated with changes in the number of neocortical neurons and microglia (Fig. 3). We estimated cell density using densitometry or estimated the total number of cells using a stereological approach. The density of immature neocortical doublecortin (DCX)⁺ neurons in E13.5 mice did not change between genotypes (Fig. 3A-B). However, the total number of Iba1⁺ microglia and the number of ramified Iba1⁺ microglia in the cortex of E13.5 mice were significantly lower in TNF^{-/-} than WT mice, just as the percentage of ramified Iba1⁺ microglia of all Iba1⁺ microglia was lower in TNF^{-/-} compared to WT mice (Fig. 3C-D). In the cortex at P7, the number of TB⁺ neurons were higher in TNF^{-/-} compared to WT mice (Fig. 3E), whereas microglia were significantly fewer (Fig. 3F). In adult TNF^{-/-} mice, the number of TB⁺ neurons was significantly increased (Fig. 3G) and the number of CD11b⁺ microglia decreased (Fig. 3H), in line with our previous report (Lambertsen et al., 2009). Following long-term treatment (2 months) with TNF inhibitors, we found no differences in cortical microglia numbers, suggesting that long-term treatment with XPro1595 or etanercept does not affect microglial numbers in the healthy, adult C57BL/6 mouse brain (Fig. 3I-J).

3.4. TNF affects microglial phagocytosis

Since developmental TNF deficiency resulted in decreased number of neocortical microglia and an increased number of neurons, we next investigated whether deficiency in either solTNF and tmTNF or solTNF only affected microglial phagocytosis following LPS activation (Fig. 4A). At day 1 after LPS stimulation, we found that 100 and 200 ng/mL XPro1595 significantly increased the number of phagocytosed beads/cells compared to control, to LPS stimulation only, and to LPS + 100 or 200 ng/mL etanercept (Fig. 4B). In contrast, etanercept treatment completely blocked phagocytosis (Fig. 4B). Cell area (Fig. 4C), perimeter length (Fig. 4D), and membrane irregularity (Fig. 4E) increased significantly following LPS and LPS + XPro1595 treatment, whereas etanercept completely blocked these changes in cell morphology (Fig. 4C-E). This suggests that TNF is essential for microglial phagocytosis, and that ablating solTNF may even increase phagocytosis.

3.5. TNF deficiency or long-term inhibition of TNF has no effect on body weight

At P7, body weights of WT mice ($4.01 \text{ g} \pm 0.15 \text{ g}$, n = 8) and TNF^{-/-} mice ($3.58 \text{ g} \pm 0.50 \text{ g}$, n = 9) did not differ between genotypes (p = 0.06, Student's unpaired t-test), and growth rate of saline, XPro1595, or etanercept treated mice was comparable between

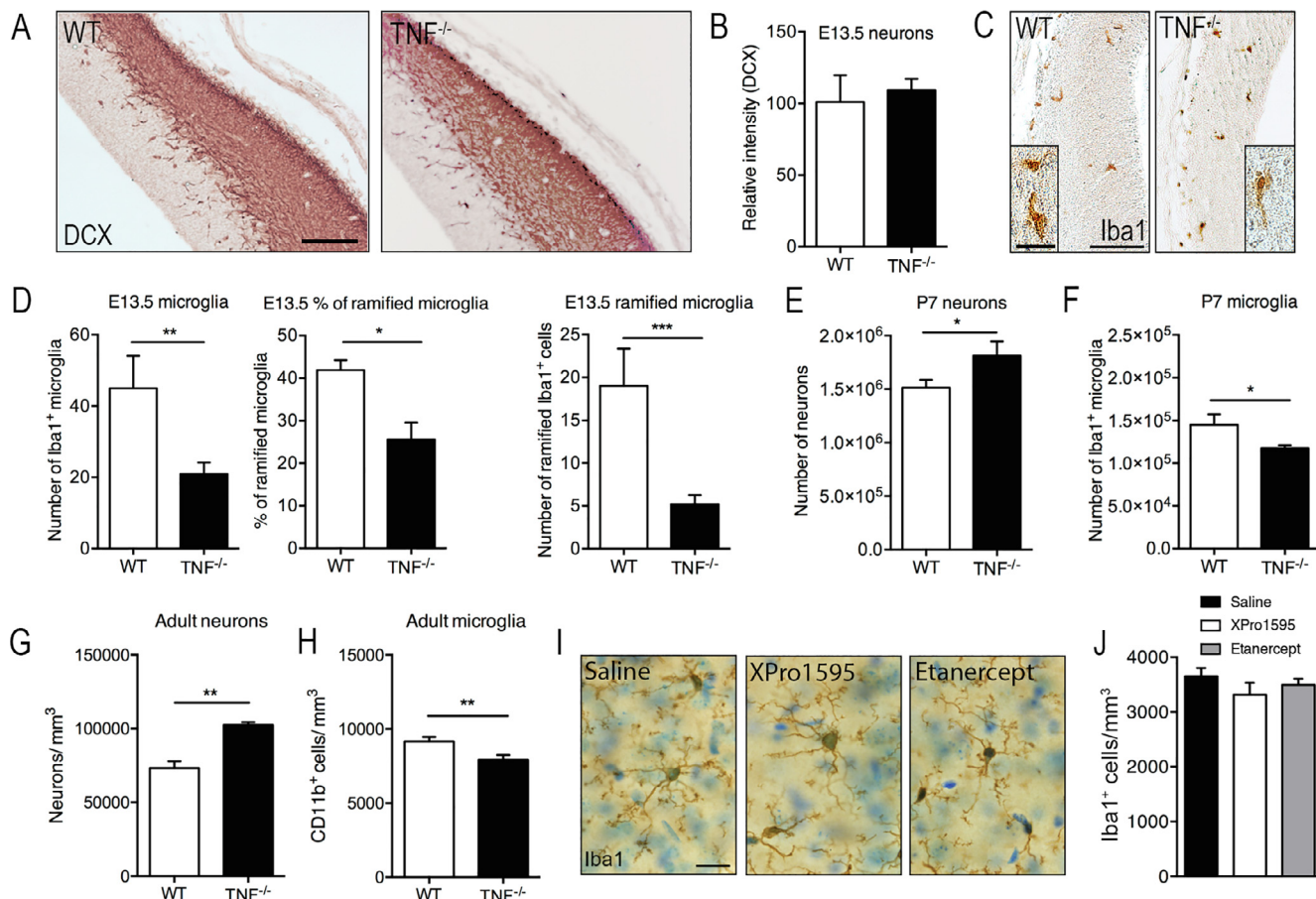


Fig. 3. TNF deficiency alters the cortical cell composition. (A) DCX⁺ staining in E13.5 mice, scalebar = 100 μm . (B) The relative intensity of DCX⁺ cells in developing neocortex was comparable in E13.5 WT and TNF^{-/-} mice (3/group). (C) Iba1⁺ cells in the developing neocortex of E13.5 mice, scalebar = 100 μm and 20 μm (high magnification). (D) Number and percentage of Iba1⁺ cells in cortex of WT and TNF^{-/-} E13.5 mice (3–10/group). (E) Number of TB⁺ neurons in neocortex of WT and TNF^{-/-} P7 mice (5/group). (F) Number of Iba1⁺ microglia in cortex of WT and TNF^{-/-} P7 mice (5/group). (G) Number of TB⁺ neurons in cortex of adult WT and TNF^{-/-} mice (6/group). (H) Number of CD11b⁺ cells in neocortex of adult WT and TNF^{-/-} mice (6/group). (I) Iba1⁺ microglia in mice treated with saline, XPro1595, or etanercept, scalebar = 20 μm . (J) Number of Iba1⁺ microglia in cortex of adult saline-, XPro1595-, and etanercept-treated mice (7–8/group). *p ≤ 0.05, **p < 0.01, Student's t-test or one-way ANOVA with Tukey's post hoc.

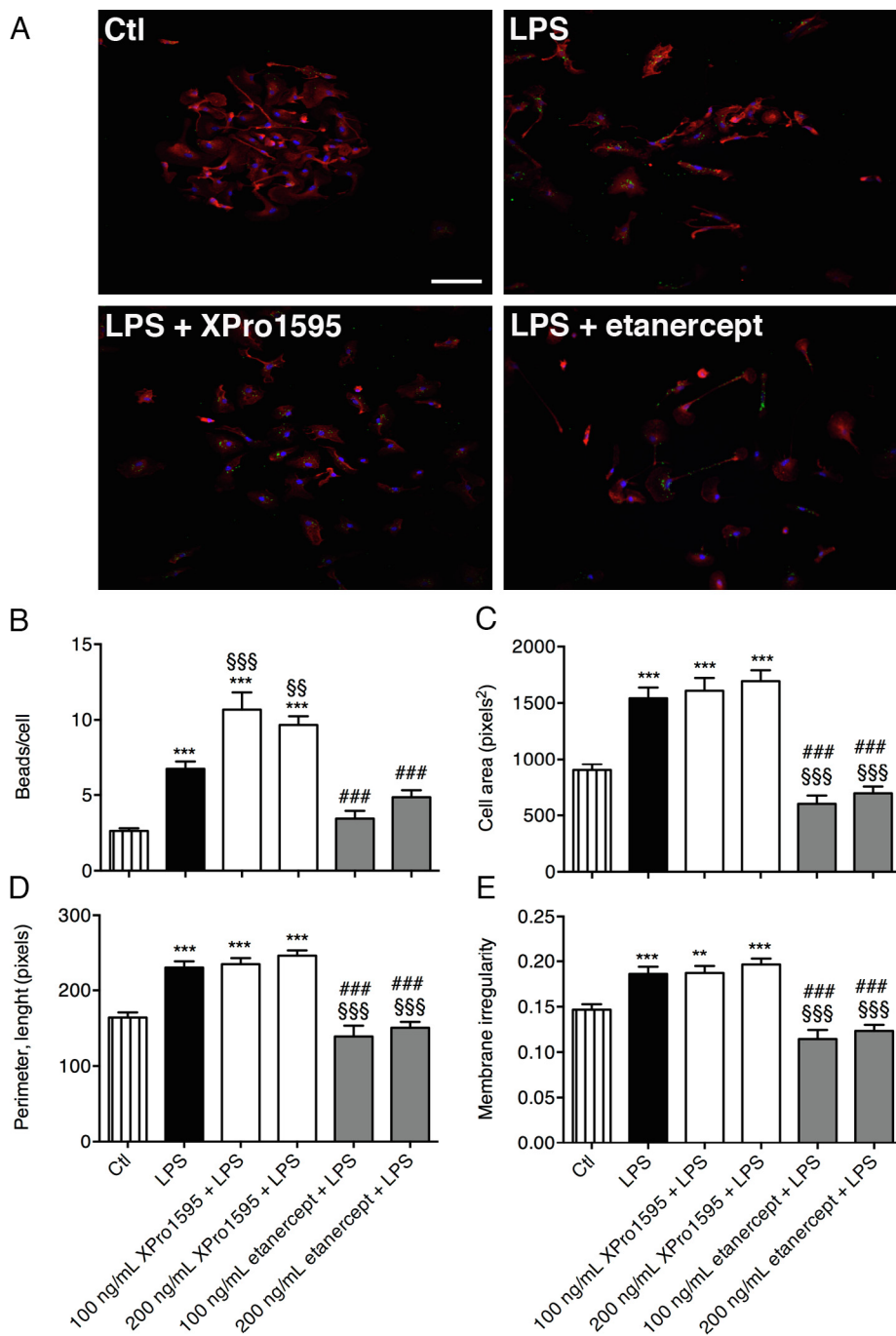


Fig. 4. TNF depletion impairs phagocytosis. (A) Primary cultures stained for Iba1 (red) and DAPI (blue) demonstrating phagocytosis of FluoSpheres Carboxylate-Modified Microspheres (green). Scale bar = 80 μ m. (B) Engulfed beads/cell in Ctl microglia ($n = 54$) and in LPS ($n = 53$), LPS + 100 ng/mL ($n = 32$) or 200 ng/mL ($n = 35$) XPro1595, and LPS + 100 ng/mL ($n = 9$) or 200 ng/mL ($n = 20$) etanercept treated microglia. (C-E) Morphological features of microglia before and after LPS stimulation with and without XPro1595 or etanercept. (C) Cell area. (D) Perimeter length. (E) Membrane irregularity. One-way ANOVA with Tukey's post hoc test. *** $p < 0.001$, ** $p < 0.01$. Asterisks (*) indicate significant differences compared to Ctl, hashtags (#) indicates significant differences compared to XPro1595 treatment, and the double-s (§) indicates significant differences compared to LPS treatment. Ctl, control; Etan, etanercept; LPS, lipopolysaccharide; XPro, XPro1595. (For interpretation of the references to color in this figure legend, the reader is referred to the web version of this article.)

treatment groups, although weights increased significantly over time (two-way ANOVA: time $p < 0.0001$ $F_{18,594} = 72.82$; treatment $p = 0.15$ $F_{2,33} = 2.00$; interaction $p = 0.97$ $F_{3,594} = 0.60$). This supports earlier findings that genetic ablation of solTNF has no effect on body weight (Madsen et al., 2016).

3.6. TNF deficiency does not affect BBB permeability

Interaction of TNF with cerebral endothelial cells can affect para-cellular permeability of the BBB, including changes in tight junction protein expression (reviewed in (Pan and Kastin, 2007)). To assess the effect of TNF deficiency on BBB permeability, we evaluated albumin leakage into the CNS parenchyma (Fig. 5A-B), the expression of the tight junction protein claudin-5 (Fig. 5C-D) and the glucose transporter GLUT1 (Fig. 5E-F). Expression of all of these molecules, quantified by

measuring the relative staining intensity, was comparable between E13.5 WT and TNF^{-/-} mice (Fig. 5B,D,F), suggesting that TNF deficiency does not affect the BBB under non-inflammatory conditions.

3.7. Two months of TNF-inhibitor treatment has no effect on plasma cytokines

To see whether long-term TNF inhibition altered circulating cytokine levels, we measured plasma expression levels of TNF, IL-1 β , IL-6, IFN γ , CXCL1, IL-10, IL-12p70, IL-2, IL-4, and IL-5 two months after onset of saline, XPro1595, or etanercept treatment. XPro1595 for two months significantly upregulated TNF levels (Fig. 6A), but we observed no effect of XPro1595 or etanercept on other plasma cytokines (Fig. 6B-J).

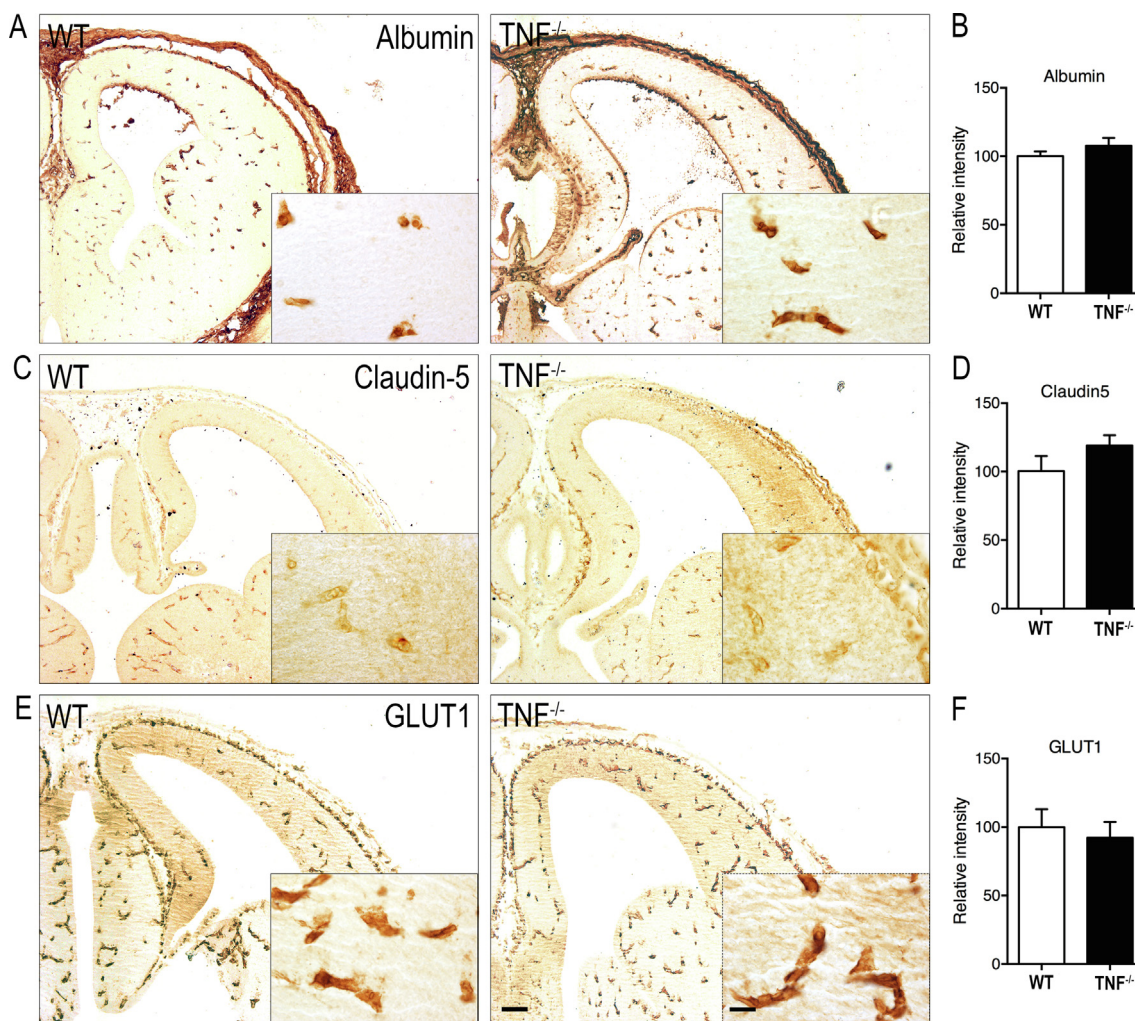


Fig. 5. TNF deficiency does not compromise BBB permeability. (A) Albumin staining in E13.5 WT and $\text{TNF}^{-/-}$ mice. (B) Relative intensity of albumin in the developing neocortex of E13.5 WT and $\text{TNF}^{-/-}$ mice (7–11/group). (C) Claudin-5 staining in E13.5 WT and $\text{TNF}^{-/-}$ mice. (D) Relative intensity of claudin-5 in the developing neocortex of E13.5 WT and $\text{TNF}^{-/-}$ mice (3–13/group). (E) GLUT1 staining in E13.5 WT and $\text{TNF}^{-/-}$ mice. (F) Relative intensity of GLUT1 in the developing neocortex of E13.5 WT and $\text{TNF}^{-/-}$ mice (3–7/group). Scalebars = 100 μm and 10 μm (insert). Student's *t*-test.

3.8. TNF deficiency alters monoamine levels and turnover rates

Previous findings on the role of TNF in learning and memory (Golan et al., 2004a), the observed alterations in the monoamine pathways (Fig. 1B), and the downregulation of Comt1 mRNA expression in the brain of $\text{TNF}^{-/-}$ mice (Fig. 1C) prompted us to investigate possible changes in the levels of monoamines and their metabolites in various brain areas by HPLC (Table 3 and Supplementary table 2). No differences in 5-HT levels were observed in any of the measured brain regions (Supplementary table 2). However, developmental TNF deficiency increased 5-HT turnover in hippocampus, brainstem, and cerebellum, giving higher 5-HIAA levels in hippocampus and brainstem and a higher 5-HT turnover in cerebellum (based on an elevated 5-HIAA/5-HT ratio). 5-HIAA was upregulated in the striatum of $\text{TNF}^{-/-}$ mice without a change in the turnover rate (Table 3 and Supplementary table 2). Dopamine levels were similar in WT and $\text{TNF}^{-/-}$ mice in all brain regions (Supplementary table 2). The metabolite DOPAC was lower in the prefrontal cortex of $\text{TNF}^{-/-}$ mice, and upregulated in the brain stem (Table 3). The DOPAC/DA turnover ratio was increased in hippocampus and brainstem. HVA was upregulated in the striatum of $\text{TNF}^{-/-}$ mice, and the HVA/DA turnover ratio was increased in striatum and occipital cortex of $\text{TNF}^{-/-}$ mice. NA levels did not differ between genotypes (Supplementary table 2). Levels of DA, DOPAC and HVA are usually very low in the cerebellum, often below detection

limits, and were thus omitted from the statistical analysis.

3.9. Non-selective TNF inhibition causes learning impairment

Both developmental TNF deficiency and long-term TNF inhibition altered the number of proliferating cells in the adult mouse brain. As neurogenesis in the dentate gyrus of the hippocampus has been linked to learning and memory functions, we performed a spatial learning and memory retention test (Barnes maze) in adult $\text{TNF}^{-/-}$ versus WT mice (Fig. 7A–C) and in adult C57BL/6 mice treated long-term with saline, XPro1595, or etanercept (Fig. 7D–F). When comparing WT and $\text{TNF}^{-/-}$ mice, WT mice learned the task over time, as shown by the reduced latency (time) to find the goal box at day 3 and day 4 as compared to day 1 (Fig. 7A). $\text{TNF}^{-/-}$ mice found the goal box rapidly during all four days of the learning phase (Fig. 7A). Already on day 1, $\text{TNF}^{-/-}$ quickly found the hidden goal box, at which time point the $\text{TNF}^{-/-}$ mice displayed significantly decreased latency time to find the hidden goal box compared to WT mice (Fig. 7B). On day 5 the goal box was removed. During the first four trials on day 5, the visual cues were placed similarly as on days 1 to 4. On the fifth trial, the cues were placed randomly to test memory retention. The mice exhibited comparable memory retention patterns (Fig. 7C), spending equal time in the quadrant zones ($p = 0.19$).

We then tested adult C57BL/6 mice after long-term exposure to TNF

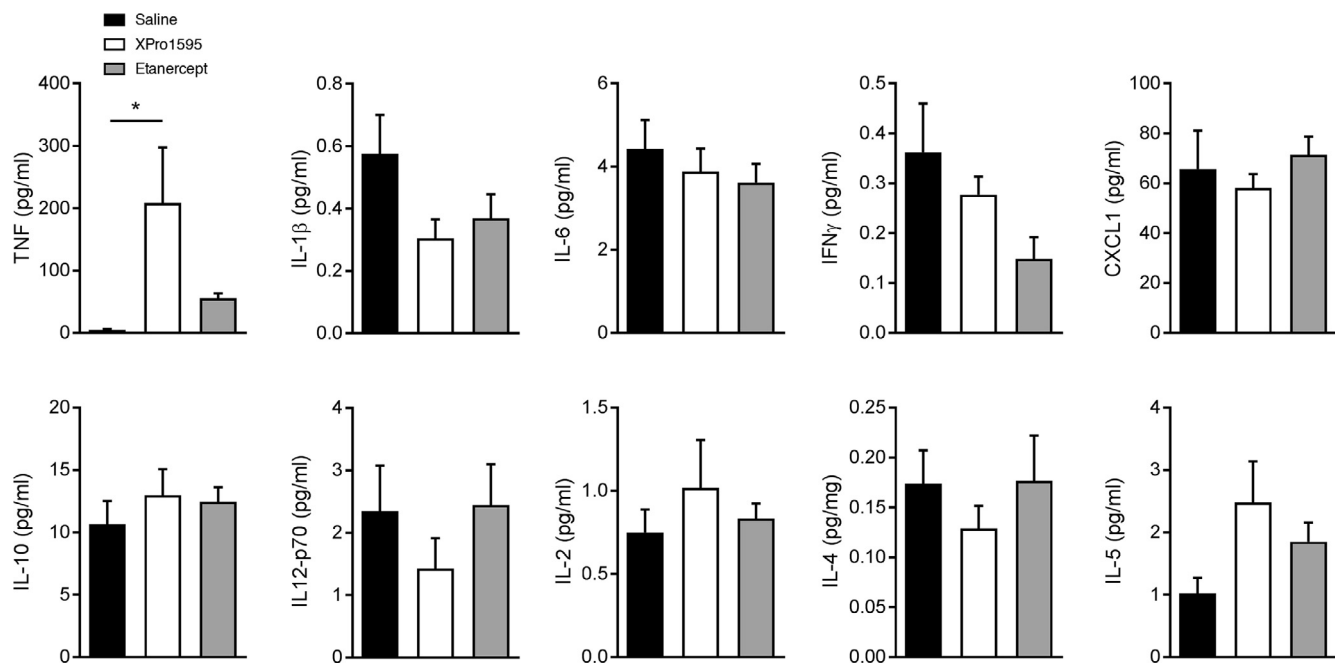


Fig. 6. Plasma cytokine profile after two months of treatment with saline, XPro1595, or etanercept. Plasma levels of TNF (A), IL-1 β (B), IL-6 (C), interferon-gamma (IFN γ) (D), CXCL1 (E), IL-10 (F), IL-12p70 (G), IL-1 (H), IL-4 (I), and IL-5 (J) (7–8 mice/group), *p ≤ 0.05, one-way ANOVA with Tukey's post hoc test.

Table 3
HPLC analysis of monoamines.

	P-value	TNF ^{+/+} Mean pmol/mg wet tissue ± SEM (n)	TNF ^{-/-} Mean pmol/mg wet tissue ± SEM (n)
5-HIAA/5-HT			
Prefrontal cortex	0.97	0.28 ± 0.03 (6)	0.28 ± 0.03 (5)
Occipital cortex	0.19	0.60 ± 0.07 (6)	0.81 ± 0.13 (6)
Striatum	0.07	0.63 ± 0.04 (6)	0.73 ± 0.01 (6)
Hippocampus	***0.001	0.50 ± 0.02 (6)	0.69 ± 0.04 (6)
Thalamus + Hypothalamus	0.69	0.72 ± 0.06 (6)	0.69 ± 0.02 (5)
Brainstem	**0.008	0.66 ± 0.02 (6)	0.79 ± 0.03 (6)
Cerebellum	*0.02	0.93 ± 0.05 (6)	1.21 ± 0.08 (6)
DOPAC/DA			
Prefrontal cortex	0.17	0.89 ± 0.06 (5)	0.63 ± 0.14 (6)
Occipital cortex	0.08	0.55 ± 0.09 (6)	1.60 ± 0.66 (4)
Striatum	0.17	0.06 ± 0.00 (5)	0.07 ± 0.00 (5)
Hippocampus	* < 0.05	1.65 ± 0.41 (5)	4.05 ± 1.08 (3)
Thalamus + Hypothalamus	0.73	0.35 ± 0.08 (6)	0.31 ± 0.06 (5)
Brainstem	**0.007	0.44 ± 0.02 (6)	0.51 ± 0.01 (6)
Cerebellum	N/A	N/A	N/A
HVA/DA			
Prefrontal cortex	N/A	N/A	N/A
Occipital cortex	*0.04	0.38 ± 0.10 (6)	1.19 ± 0.38 (4)
Striatum	****0.0001	0.09 ± 0.01 (5)	0.14 ± 0.00 (5)
Hippocampus	0.51	1.36 ± 0.55 (5)	2.18 ± 1.13 (4)
Thalamus + Hypothalamus	0.43	0.33 ± 0.07 (6)	0.45 ± 0.13 (6)
Brainstem	N/A	N/A	N/A
Cerebellum	0.66	1.06 ± 0.20 (6)	1.24 ± 0.33 (6)

5-HT, 5-hydroxytryptamine; 5-HIAA, 5-hydroxyindoleacetic acid; DA, dopamine; DOPAC, 3,4-dihydroxyphenylacetic acid; HVA, homovanillic acid. *p < 0.05, **p < 0.01, ***p < 0.001, ****p < 0.0001.

inhibitors. Both saline- and XPro1595-treated mice showed improved learning as they were significantly faster in finding the hidden goal box on day 2, 3, and 4 compared to day 1 (Fig. 7D). XPro1595-treated mice showed improved learning over time (Fig. 7D). This was not observed in the etanercept-treated group, indicating impaired learning (Fig. 7D). The etanercept-treated mice also took significantly more time to find

the goal box on days 3 and 4 compared to the saline- and XPro1595-treated mice (Fig. 7E). The treatment groups spent similar amounts of time searching for the goal box on day 5, excluding trial 4 when XPro1595-treated mice spent more time than the others in target zone, and etanercept-treated mice spent more time in opposite zone than XPro1595-treated mice (Fig. 7F). Etanercept-treated mice thus displayed impaired learning curve on the Barnes maze, but memory retention on day 5 was comparable in the three groups.

3.10. TNF deficiency has no effect on activity, anxiety-related behavior, or exploratory behavior

Effects of developmental TNF deficiency on activity, anxiety-related behavior, and exploratory behavior in adult mice were assessed by testing WT and TNF^{-/-} mice on the Y maze and elevated plus maze. TNF deficiency had no effect on locomotor activity when measured as the travelled distance in the elevated plus maze (Fig. 8A). There were no differences between the genotypes in the time the mice spent in the open or closed arm (Fig. 8B), suggesting that developmental TNF deficiency has no effect on anxiety-related behavior of the mice, nor were there differences in spontaneous alternation behavior between WT and TNF^{-/-} mice (Fig. 8C), suggesting that the working memory of the mice was intact.

To test whether the impaired learning of etanercept-treated mice (Fig. 7D) was due to a lack of natural anxiety-related behavior, we evaluated characteristics associated with anxiety-related behavior in the open field test after treatment with saline, XPro1595, or etanercept. First, we measured the total travel distance of the animals during the test to exclude the possibility that the treatment affected their locomotor activity. We found no differences in the total distance travelled between mice treated for one and two months in any of the groups (Fig. 8D). In the open field test, saline- and XPro1595-treated animals had significantly fewer entries into the center zone after two months of treatment than after one month of treatment (Fig. 8E). The center-perimeter ratio decreased significantly in all three groups between one and two months of treatment (Fig. 8F). The number of dropped fecal boli was comparable between the treatment groups after one and two months of treatment (Fig. 8G). The time spent in the wall zone increased in all treatment groups, and the time spent in the center zone

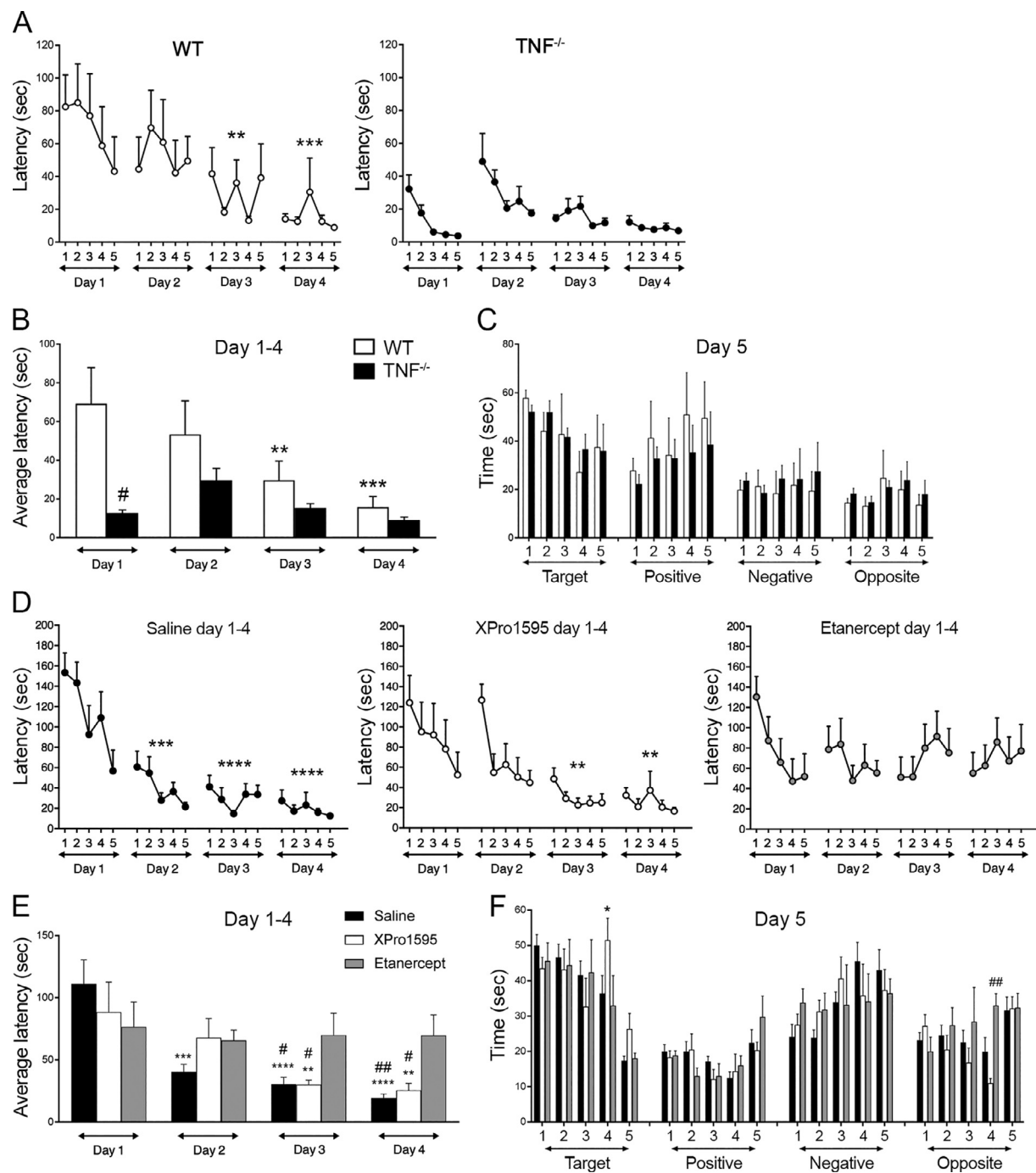


Fig. 7. Barnes maze spatial learning and memory retention test. (A) Learning curve of WT and TNF^{-/-} mice presented as latency (time) to find the goal box in each trial (7–8 mice/group), **p < 0.01, ***p < 0.001 compared to average latency on day 1, two-way ANOVA with Tukey's *post hoc* test. (B) Average latency to find a goal box on days 1 to 4. *p < 0.05, **p < 0.01, ***p < 0.001 compared to average latency on day 1 within the genotype; two-way ANOVA with Tukey's *post hoc* test; #p ≤ 0.05 compared to average latency between genotypes; Student's unpaired *t*-test. (C) Time spent on different zones of the Barnes maze on day 5. (D) Learning curve of saline-, XPro1595-, and etanercept-treated mice (8/group), **p < 0.01, ***p < 0.001, ****p < 0.0001 compared to average latency on day 1; two-way ANOVA with Tukey's *post hoc* test. (E) Average latency to find a goal box, **p < 0.01, ***p < 0.001, ****p < 0.0001 compared to average latency on day 1 within the genotype; two-way ANOVA with Tukey's *post hoc* test; #p ≤ 0.05, #p < 0.01 compared to average latency between genotypes, one-way ANOVA with Tukey's *post hoc* test. (F) Time spent in different zones on day 5, *p ≤ 0.05 for XPro1595-treated mice compared to saline- and etanercept-treated mice in target zone on trial 4; ##p < 0.01 for etanercept-treated mice compared to XPro1595-treated mice in opposite zone on trial 4; two-way ANOVA with Sidak's multiple comparisons test.

decreased in all treatment groups between one and two months of treatment (Fig. 8H), suggesting that etanercept-treated mice were not anxious. Exploratory behavior measured as rearing was comparable in all groups (Fig. 8I–J). Spontaneous alternation behaviors in the Y maze were comparable between saline, XPro1595, and etanercept treated mice (Fig. 8K). In conclusion, neither developmental TNF deficiency

nor treatment with XPro1595 or etanercept had any significant effect on anxiety or exploratory behavior in adult mice.

4. Discussion

In this study, we found that TNF deficiency altered the expression of

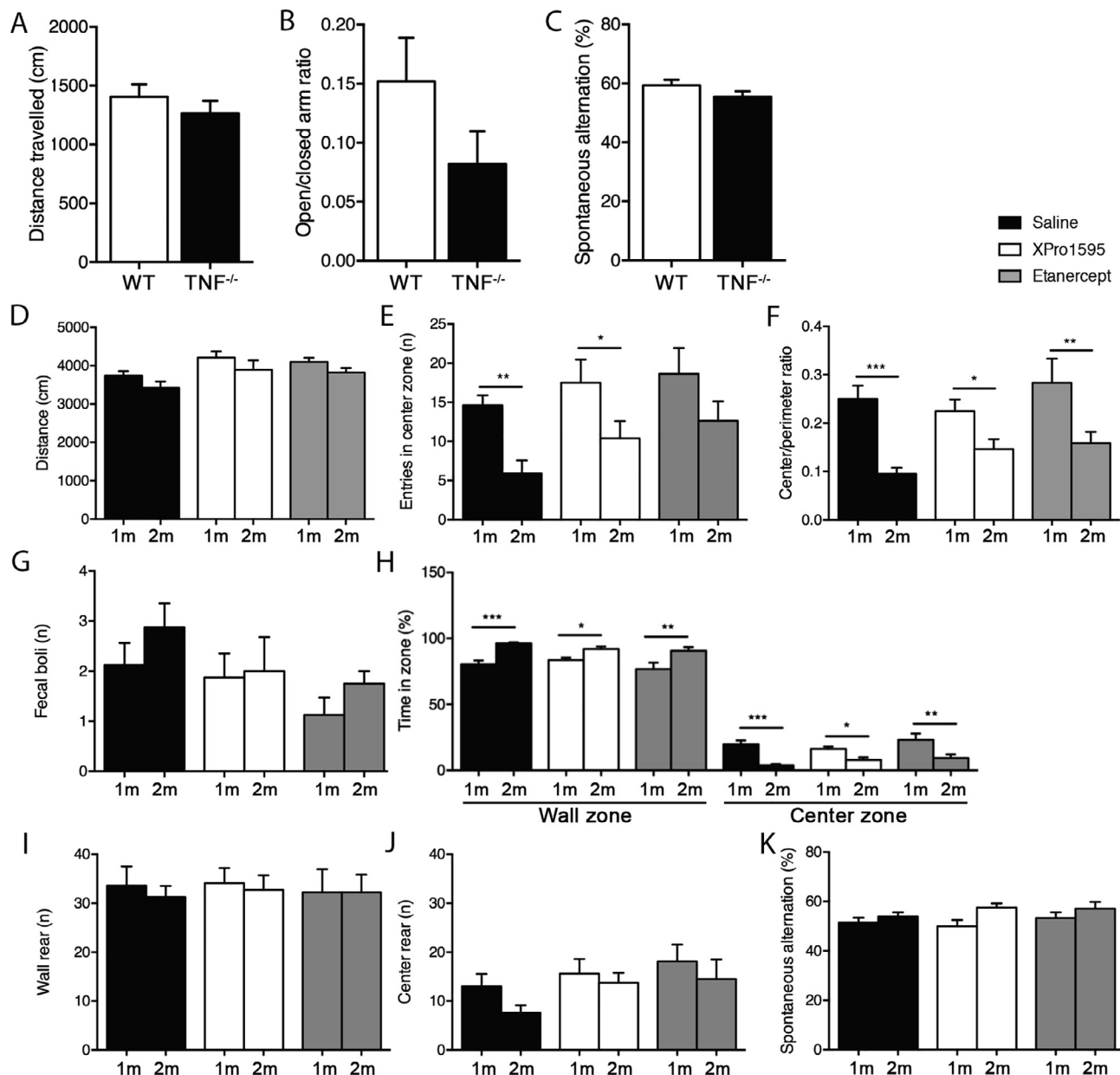


Fig. 8. TNF deficiency has no effect on anxiety or exploratory behavior in mice. (A) Locomotor activity measured as distance travelled in elevated plus maze for WT and TNF^{-/-} mice (7–9/group). (B) Anxiety-related behavior of WT and TNF^{-/-} mice measured as the open/closed arm ratio. (C) Working memory and exploratory behavior of WT and TNF^{-/-} mice measured as spontaneous alternation between the arms in the Y maze (12–16/group). (D–J) Locomotor activity and anxiety-related behavior of saline-, XPro1595-, and etanercept-treated mice measured as the travelled distance (D), entries into the center zone (E), center/perimeter ratio (F), number of dropped fecal boli (G), percentage time in wall and center zones (H), wall rearing (I), and center rearing (J) in the open field test (8/group). (K) Working memory and exploratory behavior measured as spontaneous alternation between the arms in the Y maze (8/group). *p ≤ 0.05, **p < 0.01, ***p < 0.001, Student's paired t-test.

genes and proteins related to neurogenesis and WNT signaling, which impacted the organization of the neurogenic zones and altered the composition of microglia and neurons in the neocortex of the brain. We also found that long-term inhibition of TNF with the non-selective inhibitor etanercept reduced the number of BrdU⁺ cells in the granule cell layer of the dentate gyrus and impaired learning and memory.

TNF has been shown to be important for synaptic transmission and homeostatic synaptic scaling (Beattie et al., 2002; Kaneko et al., 2008; Stellwagen and Malenka, 2006) and TNF expression regulates WNT signaling (Hiyama et al., 2013; Zhao et al., 2015). In the present study, we found that TNF deficiency regulates the expression of genes and proteins related to WNT signaling, as we observed lower levels of FZD6 and CTHRC1 in TNF^{-/-} compared to WT mice. Given the importance

of these proteins in stabilizing the WNT receptor complex, changes potentially could lead to alterations in the number of proliferating cells. Thus, we investigated the effect of TNF on cell proliferation. We found that TNF deficiency decreased cell proliferation in VZ, SEZ, and dentate gyrus during development. These findings are in agreement with studies demonstrating that TNF promotes apoptotic cell death in hippocampal cultures and in newborn hippocampal progenitor cells (Cacci et al., 2005; Zhao et al., 2001). TNF has also been shown to suppress neural progenitor cell proliferation but increases the migration *in vitro* (Ben-Hur et al., 2003); these results are at odds, however, with previous studies showing that maternal immune activation can also result in reduced proliferation in the embryonic VZ (Stolp et al., 2011) and that adult neural stem cells display impaired proliferation when exposed to

TNF (Wong et al., 2004). It is likely that the mechanisms of these proliferation changes are different, as the concentration of TNF was found to be the regulating factor in cell proliferation, with a low TNF dose increasing cell proliferation and a high dose causing cell death (Bernardino et al., 2008). In our study, we found TNF^{-/-} mice to have reduced TNFR2 mRNA expression. As earlier studies found that TNFR2 deficiency reduced neurogenesis (Chen and Palmer, 2013), the suppressive effect of TNF on cell proliferation could potentially be mediated through TNFR2, as suppression of cell proliferation promotes the differentiation of neural progenitor cells into neurons.

We found that TNF not only regulated cell proliferation in the neurogenic niche but also altered microglial and neuronal numbers in the neocortex. TNF deficiency reduced the number of microglia and increased the number of TB⁺ neurons, data which are in line with previous studies by our lab demonstrating reduced numbers of CD45^{dim}CD11b⁺ microglia in adult TNF^{-/-} mice (Lambertsen et al., 2009). Microglia are known to regulate the number of newborn neurons in the dentate gyrus by phagocytosis (Sierra et al., 2010). In TNF^{-/-} mice, the increased number of neurons could be a result of impaired microglial phagocytosis. This is supported by our findings showing that etanercept completely blocks phagocytosis in primary microglial cultures stimulated with LPS, compared to XPro1595, which results in increased phagocytosis. We have also recently shown that compared to WT microglia, microglia expressing only tmTNF display decreased expression of Methyl-CpG-binding protein 2 (MECP2) (Yli-Karjanmaa et al., 2019), a protein involved in microglia responsiveness to environmental stimuli to promote homeostasis. Therefore, given the findings that MECP2-deficient mice display decreased number of microglia compared to WT mice (Cronk et al., 2015), it is possible that solTNF, rather than tmTNF, plays a role in microgliogenesis during development.

The increased number of neurons in TNF^{-/-} mice could also be a result of the abnormally low number of microglia. Newborn neurons typically undergo extensive apoptosis during embryonic development where up to 70% of cells die before integrating into the existing neuronal circuit (Thomaidou et al., 1997). Microglia that phagocytose newborn neurons are not activated but express a ramified morphology in their unchallenged state (Sierra et al., 2010). We found a lower total number of microglia but also a lower percentage of ramified cells at E13.5, implying that fewer microglia were in a phagocytic state in TNF^{-/-} mice. In support of this, we show downregulated mRNA expression of *Lpl* in adult TNF^{-/-} mice. In CNS, *Lpl* is mainly expressed in the hippocampus, and the highest expression of *Lpl* mRNA is detected in microglia (Zhang et al., 2014; Zhang et al., 2016). Earlier studies show LPL to be an important regulator of phagocytosis and innate immunity (Gao et al., 2017). It has also been shown to support cognitive functions as in earlier studies neuronal *Lpl* knock-out mice showed increased anxiety and impaired learning and memory (Yu et al., 2015).

Microglia colonize the brain in waves. The first wave from the yolk sac to the embryo arrives before E8 and infiltrates the brain at E9, where the cells can be detected at E9.5 (Ginhoux et al., 2010). By E20, the distribution of microglia in the brain is nearly homogenous (Squarzoni et al., 2014). Angiogenesis occurs at the same time, and the BBB is formed with the endothelial cell layer developing on E10-E11. WNT signaling can regulate angiogenesis in the developing brain (Daneman et al., 2009), and the barrier can be vulnerable to environmental disturbances, depending on the local inflammatory environment and the stage of brain/vascular maturation (Blanchette and Daneman, 2015; Stolp et al., 2005; Stolp et al., 2009). Passive BBB permeability is controlled by the tight junctions connecting the endothelial cells, and any disturbance in permeability could alter microglial infiltration. To rule out developmental defects in the BBB that could account for the decrease in microglial number in TNF^{-/-} mice, we investigated the expression of a major tight junction protein, claudin-5 (Morita et al., 1999a; Morita et al., 1999b), which is expressed from E12 (Daneman et al., 2010). TNF secreted in an inflammatory environment decreases

the expression of claudin-5 both *in vivo* and *in vitro*, thereby increasing BBB permeability (Aveleira et al., 2010; Dickstein et al., 2000; Forster et al., 2008; Nishioku et al., 2010). However, claudin-5 expression was comparable between WT and TNF^{-/-} mice and further investigation of albumin leakage through capillaries and of GLUT1 expression revealed no differences between the mice. This suggests that TNF deficiency had no impact on angiogenesis or BBB permeability, which could account for the reduced microglial numbers.

In the microarray analysis and supported by RT-qPCR, we found that *Comt1* gene expression was decreased in TNF^{-/-} mice. *Comt1* encodes COMT, known to convert DA to 3-methoxytyramine or DOPAC to HVA. We did not assess 3-methoxytyramine, however, we measured levels of DA, DOPAC, and HVA. Instead of finding higher DOPAC and lower HVA levels, which is expected if COMT activity is reduced, we observed significantly increased HVA levels and HVA/DA ratio in striatum and a tendency of such increases in other brain regions. Since DOPAC/DA ratios were not different in TNF^{-/-} mice, we cannot conclude that DA turnover was altered. However, we observed increased 5-HT turnover (increased 5-HIAA/5-HT ratios) in hippocampus, brain stem, and cerebellum. This supports previous findings showing increased 5-HT and 5-HIAA in hippocampus, thalamus, medulla oblongata/pons, and cerebellum of TNF^{-/-} mice (Yamada et al., 2000). The observed changes in monoamine metabolites in this study cannot be linked to possible alterations in behavior as we observed there were no behavioral changes in TNF^{-/-} compared to WT mice. Alterations in serotonergic signaling have been linked to increased or decreased neurogenesis in the hippocampus, probably mediated by neurotrophins and cytokines (Haase and Brown, 2015). Long-term treatment with anti-depressive drugs, including selective serotonin reuptake inhibitors, increases extracellular levels of 5-HT in hippocampus (Cremers et al., 2007), reduces 5-HT turnover as assessed by reductions in 5-HIAA/5-HT ratios in brain tissue (Conti et al., 2014), and increases neurogenesis in experimental animals (Malberg et al., 2000). We observed significant increases in 5-HT turnover in hippocampus of adult TNF^{-/-} mice, which may be related to the observed reductions in proliferating cells.

Given the importance of TNF in the spatial organization of neurogenic zones and the effect of TNF deficiency on microglial and neuronal numbers, we next investigated the effect of long-term TNF inhibitor treatment on the WNT signaling proteins CTHRC1 and FZD6, cell proliferation and learning and memory in healthy adult mice. We found that mice treated with XPro1595 for two months had significantly higher expression of CTHRC1 compared to saline-treated mice, whereas treatment with etanercept had no effect. We saw the same tendency for FZD6. This suggests that tmTNF, but not solTNF, is needed for functional WNT signaling. We therefore also estimated the total number of BrdU⁺ cells in the dentate gyrus and the number of neocortical microglia after two months of TNF-inhibitor treatment. We found that long-term inhibition of TNF had no effect on neocortical microglial numbers, however, etanercept significantly reduced the number of BrdU⁺ cells in the granule cell layer of dentate gyrus. This correlated with etanercept-treated mice displaying impaired spatial learning on the Barnes maze test. As hippocampus-dependent learning can induce neurogenesis (Gould et al., 1999), we also estimated the total number of EdU⁺ cells in the dentate gyrus following Barnes maze induced learning and memory. We found, however, that neither XPro1595 nor etanercept had any effect the number of EdU⁺ proliferative cells in the dentate gyrus after the Barnes maze test. These findings suggest, that though non-selective TNF inhibition affects learning induced memory it does not affect learning-induced neurogenesis. One week of learning may, however, have been too short to detect differences in proliferative cells.

It should be mentioned that the present studies using TNF inhibitors were done in healthy animals under normal brain homeostasis where TNF is constitutively released at physiological relevant levels to keep proper synaptic plasticity. In contrast, when central TNF levels dramatically increase, the synaptic action of TNF remarkably interferes

with brain circuits of learning and cognition and contributes to excitotoxicity and neurodegeneration. Multiple sclerosis (MS) and Alzheimer's disease (AD) are prototypical neuro-inflammatory and -degenerative diseases in which inflammation triggers excitotoxic mechanisms contributing to neurodegeneration and in which TNF is chronically increased (Rossi et al., 2014; Tarkowski et al., 2003). In this scenario, TNF starts to exert noxious effects on synaptic transmission and to account for effects associated with memory and learning deficits (reviewed in (Chang et al., 2017)). In experimental animal models of MS and AD, it has been shown that peripheral inhibition of solTNF using XPro1595 attenuates disease, cognitive and long-term potentiation deficits (Brambilla et al., 2011; MacPherson et al., 2017; Taoufik et al., 2011).

Non-selective TNF inhibitors such as etanercept are currently used to treat patients suffering from peripheral chronic inflammatory diseases, such as rheumatoid arthritis (RA) and inflammatory bowel disease (IBD), where these drugs successfully reduce the excessive detrimental TNF levels associated with these diseases. In RA and sarcoidosis patients, treated with non-selective TNF inhibitors, cognition significantly improved (Chen et al., 2010; Elfferich et al., 2010). Furthermore, in IBD patients, the incidence of Parkinson's disease in patients treated with non-selective TNF inhibitors significantly decreased (Peter et al., 2018) and in RA patients, the incidence of AD decreased (Chou et al., 2016). This clearly indicates a beneficial effect of anti-TNF treatment on brain function in patients suffering from chronic inflammatory diseases. It should be mentioned, however that treatment with non-selective TNF inhibitors in these patients can be associated with neurological side effects such as demyelinating diseases (reviewed in (Scheinfeld, 2004)). Whether XPro1595 has a potential advantage over etanercept in these patients remains to be clarified. As we in the present study did not investigate the possible effects of TNF inhibition on synaptic pruning and other memory formation processes, it is unclear how XPro1595 and etanercept would alter brain wiring processes during adolescence. Also, whether XPro1595 has a potential advantage over etanercept on the spatial organization of the neurogenic zones and on microglial and neuronal numbers during development and in adolescent under chronic neuroinflammatory conditions remains to be clarified.

In conclusion, we show that developmental TNF deficiency decreases the number of neocortical microglia and increases the number of neocortical neurons. We also report that long-term use of non-selective TNF inhibitors in healthy, adult mice can alter neurogenic zones and impair learning and memory.

5. Authors' contributions

MY-K and KSL performed experiments, interpreted data, and performed statistical analysis, and helped write the manuscript. LKK and JBG performed HPLC experiments. HS, AB, and DCA performed parts of the embryonic study. SLC and MY-K performed BrdU and EdU cell countings. PVN and MCL performed the primary microglia studies. BF performed parts of the P7 study and assisted with real-time RT-qPCR analysis together with LHF, JS, NAM, and CDF. LN, PTJ, and CDF performed microarray analysis. MM assisted with parts of the embryonic and P7 experiments and gave constructive input to the study. RB assisted with parts of the TNF inhibitor studies. KLL conceived the study, performed experiments, interpreted data, performed statistical analysis and wrote the manuscript. All authors read and approved the manuscript.

Acknowledgements

David E. Szymkowski (Xencor Inc, Monrovia, USA) is acknowledged for generous donation of XPro1595. Yvonne Couch and Matt Evans are acknowledged for assistance with collection of E13.5 tissue. Alexander Viftrup Andersen is acknowledged for developing PuntoCalc. Sussanne

Petersen, Dorte Lyholmer, and Ulla Damgaard Munk are acknowledged for skilled technical assistance. This work was supported by the Danish Council for Independent Research, Medical Sciences (DFF-4183-00033 to KLL), the Lundbeck Foundation (R54-A5539 and R173-2014-955 to KLL), Fonden til Laegevidenskabens Fremme (to MYK), and Overlaegeraadets Legatudvalg (to MYK).

Appendix A. Supplementary data

Supplementary data to this article can be found online at <https://doi.org/10.1016/j.bbi.2019.08.195>.

References

- Aarum, J., Sandberg, K., Hauberlein, S.L., Persson, M.A., 2003. Migration and differentiation of neural precursor cells can be directed by microglia. *Proc. Natl. Acad. Sci. U.S.A.* 100, 15983–15988.
- Al-Ali, H., Gao, H., Dalby-Hansen, C., Peters, V.A., Shi, Y., Brambilla, R., 2017. High content analysis of phagocytic activity and cell morphology with PuntoMorph. *J. Neurosci. Meth.* 291, 43–50.
- Altman, J., Das, G.D., 1965. Autoradiographic and histological evidence of postnatal hippocampal neurogenesis in rats. *J. Comp. Neurol.* 124, 319–335.
- Alvarez-Buylla, A., Lim, D.A., 2004. For the long run: maintaining germinal niches in the adult brain. *Neuron* 41, 683–686.
- Aveleira, C.A., Lin, C.M., Abcouwer, S.F., Ambrosio, A.F., Antonetti, D.A., 2010. TNF-alpha signals through PKCzeta/NF-kappaB to alter the tight junction complex and increase retinal endothelial cell permeability. *Diabetes* 59, 2872–2882.
- Bachstetter, A.D., Morganti, J.M., Jernberg, J., Schlunk, A., Mitchell, S.H., Brewster, K.W., Hudson, C.E., Cole, M.J., Harrison, J.K., Bickford, P.C., Gemma, C., 2011. Fractalkine and CX 3 CR1 regulate hippocampal neurogenesis in adult and aged rats. *Neurobiol. Aging* 32, 2030–2044.
- Barnum, C.J., Chen, X., Chung, J., Chang, J., Williams, M., Grigoryan, N., Tesi, R.J., Tansey, M.G., 2014. Peripheral Administration of the SELECTIVE INHIBITOR OF SOLUBLE TUMOR NECROSIS FACTOR (TNF) XPro(R)1595 attenuates nigral cell loss and glial activation in 6-OHDA hemiparkinsonian rats. *J. Parkinson's Dis.* 4, 349–360.
- Batchelor, P.E., Porritt, M.J., Martinello, P., Parish, C.L., Liberatore, G.T., Donnan, G.A., Howells, D.W., 2002. Macrophages and microglia produce local trophic gradients that stimulate axonal sprouting toward but not beyond the wound edge. *Mol. Cell. Neurosci.* 21, 436–453.
- Beattie, E.C., Stellwagen, D., Morishita, W., Bresnahan, J.C., Ha, B.K., Von Zastrow, M., Beattie, M.S., Malenka, R.C., 2002. Control of synaptic strength by glial TNFalpha. *Science* 295, 2282–2285.
- Bedrosian, T.A., Weil, Z.M., Nelson, R.J., 2013. Chronic dim light at night provokes reversible depression-like phenotype: possible role for TNF. *Mol. Psychiatry* 18, 930–936.
- Belarbi, K., Arellano, C., Ferguson, R., Jopson, T., Rosi, S., 2012. Chronic neuroinflammation impacts the recruitment of adult-born neurons into behaviorally relevant hippocampal networks. *Brain Behav. Immun.* 26, 18–23.
- Ben-Hur, T., Ben-Menachem, O., Furer, V., Einstein, O., Mizrahi-Kol, R., Grigoriadis, N., 2003. Effects of proinflammatory cytokines on the growth, fate, and motility of multipotential neural precursor cells. *Mol. Cell. Neurosci.* 24, 623–631.
- Bernardino, L., Agasse, F., Silva, B., Ferreira, R., Grade, S., Malva, J.O., 2008. Tumor necrosis factor-alpha modulates survival, proliferation, and neuronal differentiation in neonatal subventricular zone cell cultures. *Stem Cells* 26, 2361–2371.
- Bhanot, P., Brink, M., Samos, C.H., Hsieh, J.C., Wang, Y., Macke, J.P., Andrew, D., Nathans, J., Nusse, R., 1996. A new member of the frizzled family from Drosophila functions as a Wingless receptor. *Nature* 382, 225–230.
- Black, R.A., Rauch, C.T., Kozlosky, C.J., Peschon, J.J., Slack, J.L., Wolfson, M.F., Castner, B.J., Stocking, K.L., Reddy, P., Srinivasan, S., Nelson, N., Boiani, N., Schooley, K.A., Gerhart, M., Davis, R., Fitzner, J.N., Johnson, R.S., Paxton, R.J., March, C.J., Cerretti, D.P., 1997. A metalloproteinase disintegrin that releases tumour-necrosis factor-alpha from cells. *Nature* 385, 729–733.
- Blanchette, M., Daneman, R., 2015. Formation and maintenance of the BBB. *Mech. Dev.* 138 (Pt 1), 8–16.
- Bordiuk, O.L., Smith, K., Morin, P.J., Semenov, M.V., 2014. Cell proliferation and neurogenesis in adult mouse brain. *PLoS One* 9, e111453.
- Brambilla, R., Ashbaugh, J.J., Magliozzi, R., Dollarole, A., Karmally, S., Szymkowski, D.E., Bethea, J.R., 2011. Inhibition of soluble tumour necrosis factor is therapeutic in experimental autoimmune encephalomyelitis and promotes axon preservation and remyelination. *Brain* 134, 2736–2754.
- Butovsky, O., Talpalari, A.E., Ben-Yaakov, K., Schwartz, M., 2005. Activation of microglia by aggregated beta-amyloid or lipopolysaccharide impairs MHC-II expression and renders them cytotoxic whereas IFN-gamma and IL-4 render them protective. *Mol. Cell. Neurosci.* 29, 381–393.
- Cacci, E., Claasen, J.H., Kokkaia, Z., 2005. Microglia-derived tumor necrosis factor-alpha exaggerates death of newborn hippocampal progenitor cells in vitro. *J. Neurosci. Res.* 80, 789–797.
- Cavanagh, C., Tse, Y.C., Nguyen, H.B., Krantic, S., Breitner, J.C., Quirion, R., Wong, T.P., 2016. Inhibiting tumor necrosis factor-alpha before amyloidosis prevents synaptic deficits in an Alzheimer's disease model. *Neurobiol. Aging* 47, 41–49.
- Chang, R., Yee, K.L., Sumbria, R.K., 2017. Tumor necrosis factor alpha inhibition for

- Alzheimer's Disease. *J. Cent. Nerv. Syst. Dis.* 9: 1179573517709278.
- Chen, Y.M., Chen, H.H., Lan, J.L., Chen, D.Y., 2010. Improvement of cognition, a potential benefit of anti-TNF therapy in elderly patients with rheumatoid arthritis. *Joint Bone Spine* 77, 366–367.
- Chen, Z., Palmer, T.D., 2013. Differential roles of TNFR1 and TNFR2 signaling in adult hippocampal neurogenesis. *Brain Behav. Immun.* 30, 45–53.
- Chou, R.C., Kane, M., Ghimire, S., Gautam, S., Gui, J., 2016. Treatment for rheumatoid arthritis and risk of Alzheimer's disease: a nested case-control analysis. *CNS Drugs* 30, 1111–1120.
- Clausen, B., Degen, M., Martin, N., Couch, Y., Karimi, L., Ormhoj, M., Mortensen, M.L., Gredal, H., Gardiner, C., Sargent, I.I., Szymkowski, D.E., Petit, G.H., Deierborg, T., Finsen, B., Anthony, D., Lambertsen, K., 2014. Systemically administered anti-TNF therapy ameliorates functional outcomes after focal cerebral ischemia. *J. Neuroinflamm.* 11, 203.
- Clausen, B.H., Lambertsen, K.L., Babcock, A.A., Holm, T.H., Dagnaes-Hansen, F., Finsen, B., 2008. Interleukin-1beta and tumor necrosis factor-alpha are expressed by different subsets of microglia and macrophages after ischemic stroke in mice. *J. Neuroinflamm.* 5, 46.
- Clausen, B.H., Lambertsen, K.L., Dagnaes-Hansen, F., Babcock, A.A., von Linstow, C.U., Meldgaard, M., Kristensen, B.W., Deierborg, T., Finsen, B., 2016. Cell therapy centered on IL-1Ra is neuroprotective in experimental stroke. *Acta Neuropathol.*
- Conti, M.M., Ostock, C.Y., Lindenbach, D., Goldenberg, A.A., Kampton, E., Dell'isola, R., Katzman, A.C., Bishop, C., 2014. Effects of prolonged selective serotonin reuptake inhibition on the development and expression of L-DOPA-induced dyskinesia in hemiparkinsonian rats. *Neuropharmacology* 77, 1–8.
- Cremers, T.I., Rea, K., Bosker, F.J., Wikstrom, H.V., Hogg, S., Mork, A., Westerink, B.H., 2007. Augmentation of SSRI effects on serotonin by 5-HT2C antagonists: mechanistic studies. *Neuropsychopharmacology* 32, 1550–1557.
- Cronk, J.C., Derecki, N.C., Ji, E., Xu, Y., Lampano, A.E., Smirnov, I., Baker, W., Norris, G.T., Marin, I., Coddington, N., Wolf, Y., Turner, S.D., Aderem, A., Klibanov, A.L., Harris, T.H., Jung, S., Litvak, V., Kipnis, J., 2015. Methyl-CpG binding protein 2 regulates microglia and macrophage gene expression in response to inflammatory stimuli. *Immunity* 42, 679–691.
- Daneman, R., Agalliu, D., Zhou, L., Kuhnert, F., Kuo, C.J., Barres, B.A., 2009. Wnt/beta-catenin signaling is required for CNS, but not non-CNS, angiogenesis. *Proc. Natl. Acad. Sci. U.S.A.* 106, 641–646.
- Daneman, R., Zhou, L., Kebede, A.A., Barres, B.A., 2010. Pericytes are required for blood-brain barrier integrity during embryogenesis. *Nature* 468, 562–566.
- Danila, M.I., Patkar, N.M., Curtis, J.R., Saag, K.G., Teng, G.G., 2008. Biologics and heart failure in rheumatoid arthritis: are we any wiser? *Curr. Opin. Rheumatol.* 20, 327–333.
- Dickstein, J.B., Moldofsky, H., Hay, J.B., 2000. Brain-blood permeability: TNF-alpha promotes escape of protein tracer from CSF to blood. *American journal of physiology. Regul. Integr. Comp. Physiol.* 279, R148–R151.
- Dinarello, C.A., Cannon, J.G., Wolff, S.M., Bernheim, H.A., Beutler, B., Cerami, A., Figari, I.S., Palladino Jr., M.A., O'Connor, J.V., 1986. Tumor necrosis factor (cachectin) is an endogenous pyrogen and induces production of interleukin 1. *J. Exp. Med.* 163, 1433–1450.
- Ekdahl, C.T., 2012. Microglial activation – tuning and pruning adult neurogenesis. *Front. Pharmacol.* 3, 41.
- Ekdahl, C.T., Claessen, J.H., Bonde, S., Kokaia, Z., Lindvall, O., 2003. Inflammation is detrimental for neurogenesis in adult brain. *Proc. Natl. Acad. Sci. U.S.A.* 100, 13632–13637.
- Ekdahl, C.T., Kokaia, Z., Lindvall, O., 2009. Brain inflammation and adult neurogenesis: the dual role of microglia. *Neuroscience* 158, 1021–1029.
- Efflerich, M.D., Nelemans, P.J., Ponds, R.W., De Vries, J., Wijnen, P.A., Drent, M., 2010. Everyday cognitive failure in sarcoidosis: the prevalence and the effect of anti-TNF-alpha treatment. *Respiration* 80, 212–219.
- Ellman, D.G., Novrup, H.G., Jorgensen, L.H., Lund, M.C., Yli-Karjanmaa, M., Madsen, P.M., Vienhues, J.H., Dursun, S., Bethea, J.R., Lykke-Hartmann, K., Brambilla, R., Lambertsen, K.L., 2017. Neuronal ablation of IKK2 decreases IL-1beta levels and lesion size and improves functional outcome after spinal cord injury in mice. *JSM Neurosurg. Spine* 5, 1090.
- Ericsson, P.S., Perfilieva, E., Bjork-Eriksson, T., Alborn, A.M., Nordborg, C., Peterson, D.A., Gage, F.H., 1998. Neurogenesis in the adult human hippocampus. *Nat. Med.* 4, 1313–1317.
- Forster, C., Burek, M., Romero, I.A., Weksler, B., Couraud, P.O., Drenckhahn, D., 2008. Differential effects of hydrocortisone and TNFalpha on tight junction proteins in an *in vitro* model of the human blood-brain barrier. *J. Physiol.* 586, 1937–1949.
- Gao, H., Danzi, M.C., Choi, C.S., Taherian, M., Dalby-Hansen, C., Ellman, D.G., Madsen, P.M., Bixby, J.L., Lemmon, V.P., Lambertsen, K.L., Brambilla, R., 2017. Opposing functions of microglial and macrophagic TNFRs in the pathogenesis of experimental autoimmune encephalomyelitis. *Cell Rep.* 18, 198–212.
- Ginhoux, F., Greter, M., Leboeuf, M., Nandi, S., See, P., Gokhan, S., Mehler, M.F., Conway, S.J., Ng, L.G., Stanley, E.R., Samokhvalov, I.M., Merad, M., 2010. Fate mapping analysis reveals that adult microglia derive from primitive macrophages. *Science* 330, 841–845.
- Golan, H., Levav, T., Mendelsohn, A., Huleihel, M., 2004a. Involvement of tumor necrosis factor alpha in hippocampal development and function. *Cereb. Cortex* 14, 97–105.
- Golan, T., Yaniv, A., Bafico, A., Liu, G., Gazit, A., 2004b. The human Frizzled 6 (HFz6) acts as a negative regulator of the canonical Wnt. beta-catenin signaling cascade. *J. Biol. Chem.* 279, 14879–14888.
- Gould, E., Beylin, A., Tanapat, P., Reeves, A., Shors, T.J., 1999. Learning enhances adult neurogenesis in the hippocampal formation. *Nat. Neurosci.* 2, 260–265.
- Gransbergen, J.B., Sandberg, M., Moller Dall, A., Kornblit, B., Zimmer, J., 2002. Glutathione depletion in nigrostriatal slice cultures: GABA loss, dopamine resistance and protection by the tetrahydrobiopterin precursor sepiapterin. *Brain Res.* 935, 47–58.
- Grell, M., Douni, E., Wajant, H., Lohden, M., Clauss, M., Maxeiner, B., Georgopoulos, S., Lesslauer, W., Kollias, G., Pfizenmaier, K., Scheurich, P., 1995. The transmembrane form of tumor necrosis factor is the prime activating ligand of the 80 kDa tumor necrosis factor receptor. *Cell* 83, 793–802.
- Grell, M., Wajant, H., Zimmermann, G., Scheurich, P., 1998. The type 1 receptor (CD120a) is the high-affinity receptor for soluble tumor necrosis factor. *Proc. Natl. Acad. Sci. U.S.A.* 95, 570–575.
- Gundersen, H.J., Bendtsen, T.F., Korbo, L., Marcussen, N., Moller, A., Nielsen, K., Nyengaard, J.R., Pakkenberg, B., Sorensen, F.B., Vesterby, A., et al., 1988. Some new, simple and efficient stereological methods and their use in pathological research and diagnosis. *Apmis* 96, 379–394.
- Haase, J., Brown, E., 2015. Integrating the monoamine, neurotrophin and cytokine hypotheses of depression—a central role for the serotonin transporter? *Pharmacol. Ther.* 147, 1–11.
- Hall, A.C., Lucas, F.R., Salinas, P.C., 2000. Axonal remodeling and synaptic differentiation in the cerebellum is regulated by WNT-7a signaling. *Cell* 100, 525–535.
- Hanisch, U.K., Kettenmann, H., 2007. Microglia: active sensor and versatile effector cells in the normal and pathologic brain. *Nat. Neurosci.* 10, 1387–1394.
- Hiyama, A., Yokoyama, K., Nukaga, T., Sakai, D., Mochida, J., 2013. A complex interaction between Wnt signaling and TNF-alpha in nucleus pulposus cells. *Arthritis Res. Therapy* 15, R189.
- Hofer, S., Grandgirard, D., Burri, D., Frohlich, T.K., Leib, S.L., 2011. Bacterial meningitis impairs hippocampal neurogenesis. *J. Neuropathol. Exp. Neurol.* 70, 890–899.
- Iosif, R.E., Ekdahl, C.T., Ahlenius, H., Pronk, C.J., Bonde, S., Kokaia, Z., Jacobsen, S.E., Lindvall, O., 2006. Tumor necrosis factor receptor 1 is a negative regulator of progenitor proliferation in adult hippocampal neurogenesis. *J. Neurosci.* 26, 9703–9712.
- Kaneko, M., Stellwagen, D., Malenka, R.C., Stryker, M.P., 2008. Tumor necrosis factor-alpha mediates one component of competitive, experience-dependent plasticity in developing visual cortex. *Neuron* 58, 673–680.
- Karamita, M., Barnum, C., Mobius, W., Tansey, M.G., Szymkowski, D.E., Lassmann, H., Probert, L., 2017. Therapeutic inhibition of soluble brain TNF promotes remyelination by increasing myelin phagocytosis by microglia. *JCI Insight* 2.
- Kaster, M.P., Gadotti, V.M., Calixto, J.B., Santos, A.R., Rodrigues, A.L., 2012. Depressive-like behavior induced by tumor necrosis factor-alpha in mice. *Neuropharmacology* 62, 419–426.
- Keohane, A., Ryan, S., Maloney, E., Sullivan, A.M., Nolan, Y.M., 2010. Tumour necrosis factor-alpha impairs neuronal differentiation but not proliferation of hippocampal neural precursor cells: role of Hes1. *Mol. Cell. Neurosci.* 43, 127–135.
- Kleber, M., Sommer, L., 2004. Wnt signaling and the regulation of stem cell function. *Curr. Opin. Cell Biol.* 16, 681–687.
- Lambertsen, K.L., Clausen, B.H., Babcock, A.A., Gregersen, R., Fenger, C., Nielsen, H.H., Haugaard, L.S., Wirenfeldt, M., Nielsen, M., Dagnaes-Hansen, F., Bluthmann, H., Faergeman, N.J., Meldgaard, M., Deierborg, T., Finsen, B., 2007. Microglia and macrophages express tumor necrosis factor receptor p75 following middle cerebral artery occlusion in mice. *Neuroscience* 144, 934–949.
- Lambertsen, K.L., Clausen, B.H., Babcock, A.A., Gregersen, R., Fenger, C., Nielsen, H.H., Haugaard, L.S., Wirenfeldt, M., Nielsen, M., Dagnaes-Hansen, F., Bluthmann, H., Faergeman, N.J., Meldgaard, M., Deierborg, T., Finsen, B., 2009. Microglia protect neurons against ischemia by synthesis of tumor necrosis factor. *J. Neurosci.* 29, 1319–1330.
- Lambertsen, K.L., Deierborg, T., Gregersen, R., Clausen, B.H., Wirenfeldt, M., Nielsen, H.H., Dalmau, I., Diemer, N.H., Dagnaes-Hansen, F., Johansen, F.F., Keating, A., Finsen, B., 2011. Differences in origin of reactive microglia in bone marrow chimeric mouse and rat after transient global ischemia. *J. Neuropathol. Exp. Neurol.* 70, 481–494.
- Lambertsen, K.L., Gramsbergen, J.B., Sivasaranaparan, M., Ditzel, N., Sevelsted-Moller, L.M., Olivian-Viguera, A., Rabjerg, M., Wulff, H., Kohler, R., 2012. Genetic KCa3.1-deficiency produces locomotor hyperactivity and alterations in cerebral monoamine levels. *PLoS One* 7, e47744.
- Lambertsen, K.L., Finsen, B., Clausen, B.H., 2018. Post-stroke inflammation-target or tool for therapy? *Acta Neuropathol.*
- Lie, D.C., Colamarino, S.A., Song, H.J., Desire, L., Mira, H., Consiglio, A., Lein, E.S., Jessberger, S., Lansford, H., Dearie, A.R., Gage, F.H., 2005. Wnt signalling regulates adult hippocampal neurogenesis. *Nature* 437, 1370–1375.
- Lyck, L., Kroigard, T., Finsen, B., 2007. Unbiased cell quantification reveals a continued increase in the number of neocortical neurones during early post-natal development in mice. *Eur. J. Neurosci.* 26, 1749–1764.
- MacPherson, K.P., Sompot, P., Kannarkat, G.T., Chang, J., Sniffen, L., Wildner, M.E., Norris, C.M., Tansey, M.G., 2017. Peripheral administration of the soluble TNF inhibitor XPro1595 modifies brain immune cell profiles, decreases beta-amyloid plaque load, and rescues impaired long-term potentiation in 5xFAD mice. *Neurobiol. Dis.* 102, 81–95.
- Madsen, P.M., Clausen, B.H., Degen, M., Thyssen, S., Kristensen, L.K., Svensson, M., Ditzel, N., Finsen, B., Deierborg, T., Brambilla, R., Lambertsen, K.L., 2016. Genetic ablation of soluble tumor necrosis factor with preservation of membrane tumor necrosis factor is associated with neuroprotection after focal cerebral ischemia. *J. Cereb. Blood Flow Metab.* 36, 1553–1569.
- Malberg, J.E., Eisch, A.J., Nestler, E.J., Duman, R.S., 2000. Chronic antidepressant treatment increases neurogenesis in adult rat hippocampus. *J. Neurosci.* 20, 9104–9110.
- McCoy, M.K., Tansey, M.G., 2008. TNF signaling inhibition in the CNS: implications for normal brain function and neurodegenerative disease. *J. Neuroinflamm.* 5, 45.
- Meldgaard, M., Fenger, C., Lambertsen, K.L., Pedersen, M.D., Ladeby, R., Finsen, B., 2006. Validation of two reference genes for mRNA level studies of murine disease models in neurobiology. *J. Neurosci. Meth.*

- Mirkovic, I., Gault, W.J., Rahnama, M., Jenny, A., Gaengel, K., Bessette, D., Gottardi, C.J., Verheyen, E.M., Mlodzik, M., 2011. Nemo kinase phosphorylates beta-catenin to promote ommatidial rotation and connects core PCP factors to E-cadherin-beta-catenin. *Nat. Struct. Mol. Biol.* 18, 665–672.
- Monje, M.L., Toda, H., Palmer, T.D., 2003. Inflammatory blockade restores adult hippocampal neurogenesis. *Science* 302, 1760–1765.
- Morita, K., Furuse, M., Fujimoto, K., Tsukita, S., 1999a. Claudin multigene family encoding four-transmembrane domain protein components of tight junction strands. *Proc. Natl. Acad. Sci. U.S.A.* 96, 511–516.
- Morita, K., Sasaki, H., Furuse, M., Tsukita, S., 1999b. Endothelial claudin: claudin-5/TMVCF constitutes tight junction strands in endothelial cells. *J. Cell Biol.* 147, 185–194.
- Nishioku, T., Matsumoto, J., Dohgu, S., Sumi, N., Miyao, K., Takata, F., Shuto, H., Yamauchi, A., Kataoka, Y., 2010. Tumor necrosis factor-alpha mediates the blood-brain barrier dysfunction induced by activated microglia in mouse brain microvascular endothelial cells. *J. Pharmacol. Sci.* 112, 251–254.
- Novrup, H.G., Bracchi-Ricard, V., Ellman, D.G., Ricard, J., Jain, A., Runko, E., Lyck, L., Yli-Karjanmaa, M., Szymkowski, D.E., Pearson, P.D., Lambertsen, K.L., Bethea, J.R., 2014. Central but not systemic administration of XPro1595 is therapeutic following moderate spinal cord injury in mice. *J. Neuroinflamm.* 11, 159.
- Pan, W., Kastin, A.J., 2007. Tumor necrosis factor and stroke: role of the blood-brain barrier. *Prog. Neurobiol.* 83, 363–374.
- Paolicelli, R.C., Bolasco, G., Pagani, F., Maggi, L., Scianchi, M., Panzanelli, P., Giustetto, M., Ferreira, T.A., Guiducci, E., Dumas, L., Raguzzino, D., Gross, C.T., 2011. Synaptic pruning by microglia is necessary for normal brain development. *Science* 333, 1456–1458.
- Pasparakis, M., Alexopoulou, L., Episkopou, V., Kollias, G., 1996. Immune and inflammatory responses in TNF alpha-deficient mice: a critical requirement for TNF alpha in the formation of primary B cell follicles, follicular dendritic cell networks and germinal centers, and in the maturation of the humoral immune response. *J. Exp. Med.* 184, 1397–1411.
- Peter, I., Dubinsky, M., Bressman, S., Park, A., Lu, C., Chen, N., Wang, A., 2018. Anti-tumor necrosis factor therapy and incidence of parkinson disease among patients with inflammatory bowel disease. *JAMA Neurol.* 75, 939–946.
- Philip, R., Epstein, L.B., 1986. Tumour necrosis factor as immunomodulator and mediator of monocyte cytotoxicity induced by itself, gamma-interferon and interleukin-1. *Nature* 323, 86–89.
- Ribeiro Xavier, A.L., Kress, B.T., Goldman, S.A., Lacerda de Menezes, J.R., Nedergaard, M., 2015. A distinct population of microglia supports adult neurogenesis in the subventricular zone. *J. Neurosci.* 35, 11848–11861.
- Rossi, S., Motta, C., Studer, V., Barbieri, F., Buttari, F., Bergami, A., Sancesario, G., Bernardini, S., De Angelis, G., Martino, G., Furlan, R., Gentonze, D., 2014. Tumor necrosis factor is elevated in progressive multiple sclerosis and causes excitotoxic neurodegeneration. *Multiple Sclerosis* 20, 304–312.
- Rosso, S.B., Inestrosa, N.C., 2013. WNT signaling in neuronal maturation and synaptogenesis. *Front. Cell. Neurosci.* 7, 103.
- Ruuls, S.R., Hoek, R.M., Ngo, V.N., McNeil, T., Lucian, L.A., Janatpour, M.J., Korner, H., Scheerens, H., Hessel, E.M., Cyster, J.G., McEvoy, L.M., Sedgwick, J.D., 2001. Membrane-bound TNF supports secondary lymphoid organ structure but is subservient to secreted TNF in driving autoimmune inflammation. *Immunity* 15, 533–543.
- Saeed, A.I., Sharov, V., White, J., Li, J., Liang, W., Bhagabati, N., Braisted, J., Klapa, M., Currier, T., Thiagarajan, M., Sturm, A., Snuffin, M., Rezantsev, A., Popov, D., Ryltsov, A., Kostukovich, E., Borisovsky, I., Liu, Z., Vinsavich, A., Trush, V., Quackenbush, J., 2003. TM4: a free, open-source system for microarray data management and analysis. *Biotechniques* 34, 374–378.
- Saeed, A.I., Bhagabati, N.K., Braisted, J.C., Liang, W., Sharov, V., Howe, E.A., Li, J., Thiagarajan, M., White, J.A., Quackenbush, J., 2006. TM4 microarray software suite. *Meth. Enzymol.* 411, 134–193.
- Santiago, R.M., Baribeiro, J., Lima, M.M., Dombrowski, P.A., Andreatini, R., Vital, M.A., 2010. Depressive-like behaviors alterations induced by intranigral MPTP, 6-OHDA, LPS and rotenone models of Parkinson's disease are predominantly associated with serotonin and dopamine. *Prog. Neuro-Psychopharmacol. Biol. Psychiatry* 34, 1104–1114.
- Schafer, D.P., Lehrman, E.K., Kautzman, A.G., Koyama, R., Mardinly, A.R., Yamasaki, R., Ransohoff, R.M., Greenberg, M.E., Barres, B.A., Stevens, B., 2012. Microglia sculpt postnatal neural circuits in an activity and complement-dependent manner. *Neuron* 74, 691–705.
- Schambra, Uta B., Silver, Jerry, Lauder, Jean M., 1991. An atlas of the prenatal mouse brain: gestational day 14. *Exp. Neurol.* 114 (2), 145–183. [https://doi.org/10.1016/0014-4886\(91\)90034-A](https://doi.org/10.1016/0014-4886(91)90034-A).
- Scheinfeld, N., 2004. A comprehensive review and evaluation of the side effects of the tumor necrosis factor alpha blockers etanercept, infliximab and adalimumab. *J. Dermatolog. Treat.* 15, 280–294.
- Schneider, C.A., Rasband, W.S., Eliceiri, K.W., 2012. NIH Image to ImageJ: 25 years of image analysis. *Nat. Meth.* 9, 671–675.
- Seguin, J.A., Brennan, J., Mangano, E., Hayley, S., 2009. Proinflammatory cytokines differentially influence adult hippocampal cell proliferation depending upon the route and chronicity of administration. *Neuropsychiatr. Dis. Treat.* 5, 5–14.
- Shigemoto-Mogami, Y., Hoshikawa, K., Goldman, J.E., Sekino, Y., Sato, K., 2014. Microglia enhance neurogenesis and oligodendrogenesis in the early postnatal subventricular zone. *J. Neurosci.* 34, 2231–2243.
- Sierra, A., Encinas, J.M., Deudero, J.J., Chancey, J.H., Enikolopov, G., Overstreet-Wadiche, L.S., Tsirka, S.E., Maletic-Savatic, M., 2010. Microglia shape adult hippocampal neurogenesis through apoptosis-coupled phagocytosis. *Cell Stem Cell* 7, 483–495.
- Spalding, K.L., Bergmann, O., Alkass, K., Bernard, S., Salehpour, M., Huttner, H.B., Boström, E., Westerlund, I., Vial, C., Buchholz, B.A., Possnert, G., Mash, D.C., Druid, H., Frisen, J., 2013. Dynamics of hippocampal neurogenesis in adult humans. *Cell* 153, 1219–1227.
- Squarezoni, P., Oller, G., Hoeffel, G., Pont-Lezica, L., Rostaing, P., Low, D., Bessis, A., Ginhoux, F., Garel, S., 2014. Microglia modulate wiring of the embryonic forebrain. *Cell Rep.* 8, 1271–1279.
- Steed, P.M., Tansey, M.G., Zalevsky, J., Zhukovsky, E.A., Desjarlais, J.R., Szymkowski, D.E., Abbott, C., Carmichael, D., Chan, C., Cherry, L., Cheung, P., Chirino, A.J., Chung, H.H., Doberstein, S.K., Eivazi, A., Filikov, A.V., Gao, S.X., Hubert, R.S., Hwang, M., Hyun, L., Kashi, S., Kim, A., Kim, E., Kung, J., Martinez, S.P., Muchhal, U.S., Nguyen, D.H., O'Brien, C., O'Keefe, D., Singer, K., Vafa, O., Vielmetter, J., Yoder, S.C., Dahiyat, B.I., 2003. Inactivation of TNF signaling by rationally designed dominant-negative TNF variants. *Science* 301, 1895–1898.
- Stellwagen, D., Malenka, R.C., 2006. Synaptic scaling mediated by glial TNF-alpha. *Nature* 440, 1054–1059.
- Stolp, H.B., Dziegielewska, K.M., Ek, C.J., Habgood, M.D., Lane, M.A., Potter, A.M., Saunders, N.R., 2005. Breakdown of the blood-brain barrier to proteins in white matter of the developing brain following systemic inflammation. *Cell Tissue Res.* 320, 369–378.
- Stolp, H.B., Ek, C.J., Johansson, P.A., Dziegielewska, K.M., Bethge, N., Wheaton, B.J., Potter, A.M., Saunders, N.R., 2009. Factors involved in inflammation-induced developmental white matter damage. *Neurosci. Lett.* 451, 232–236.
- Stolp, H.B., Turnquist, C., Dziegielewska, K.M., Saunders, N.R., Anthony, D.C., Molnar, Z., 2011. Reduced ventricular proliferation in the foetal cortex following maternal inflammation in the mouse. *Brain* 134, 3236–3248.
- Taoufik, E., Tsevelevi, V., Chu, S.Y., Tselios, T., Karin, M., Lassmann, H., Szymkowski, D.E., Probert, L., 2011. Transmembrane tumour necrosis factor is neuroprotective and regulates experimental autoimmune encephalomyelitis via neuronal nuclear factor-kappaB. *Brain* 134, 2722–2735.
- Tarkowski, E., Andreassen, N., Tarkowski, A., Blennow, K., 2003. Intrathecal inflammation precedes development of Alzheimer's disease. *J. Neurol. Neurosurg. Psychiatry* 74, 1200–1205.
- Thomaidou, D., Miocene, M.C., Cavanagh, J.F., Parnavelas, J.G., 1997. Apoptosis and its relation to the cell cycle in the developing cerebral cortex. *J. Neurosci.* 17, 1075–1085.
- Tusher, V.G., Tibshirani, R., Chu, G., 2001. Significance analysis of microarrays applied to the ionizing radiation response. *Proc. Natl. Acad. Sci. U.S.A.* 98, 5116–5121.
- Tyring, S., Gottlieb, A., Papp, K., Gordon, K., Leonardi, C., Wang, A., Lalla, D., Woolley, M., Jahreis, A., Zitnik, R., Celli, D., Krishnan, R., 2006. Etanercept and clinical outcomes, fatigue, and depression in psoriasis: double-blind placebo-controlled randomised phase III trial. *Lancet* 367, 29–35.
- Vukovic, J., Colditz, M.J., Blackmore, D.G., Ruitenberg, M.J., Bartlett, P.F., 2012. Microglia modulate hippocampal neural precursor activity in response to exercise and aging. *J. Neurosci.* 32, 6435–6443.
- Walton, N.M., Sutter, B.M., Laywell, E.D., Levkoff, L.H., Kearns, S.M., Marshall 2nd, G.P., Scheffler, B., Steindler, D.A., 2006. Microglia instruct subventricular zone neurogenesis. *Glia* 54, 815–825.
- Wong, G., Goldshmit, Y., Turnley, A.M., 2004. Interferon-gamma but not TNF alpha promotes neuronal differentiation and neurite outgrowth of murine adult neural stem cells. *Exp. Neurol.* 187, 171–177.
- Yamada, K., Iida, R., Miyamoto, Y., Saito, K., Sekikawa, K., Seishima, M., Nabeshima, T., 2000. Neurobehavioral alterations in mice with a targeted deletion of the tumor necrosis factor-alpha gene: implications for emotional behavior. *J. Neuroimmunol.* 111, 131–138.
- Yamamoto, S., Nishimura, O., Misaki, K., Nishita, M., Minami, Y., Yonemura, S., Tarui, H., Sasaki, H., 2008. Ctrc1 selectively activates the planar cell polarity pathway of Wnt signaling by stabilizing the Wnt-receptor complex. *Dev. Cell* 15, 23–36.
- Yli-Karjanmaa, M., Clausen, B.H., Degen, M., Novrup, H.G., Ellman, D.G., Toft-Jensen, P., Szymkowski, D.E., Stensballe, A., Meyer, M., Brambilla, R., Lambertsen, K.L., 2019. Topical administration of a soluble TNF inhibitor reduces infarct volume after focal cerebral ischemia in mice. *Front. Neurosci.* 13, 781.
- Yu, T., Tassig, M.D., DiPatrizio, N.V., Astarita, G., Piomelli, D., Bergman, B.C., Dell'Acqua, M.L., Eckel, R.H., Wang, H., 2015. Deficiency of lipoprotein lipase in neurons decreases ampa receptor phosphorylation and leads to neurobehavioral abnormalities in mice. *PLoS One* 10, e0135113.
- Zhang, Y., Chen, K., Sloan, S.A., Bennett, M.L., Scholze, A.R., O'Keefe, S., Phatnani, H.P., Guarneri, P., Caneda, C., Ruderisch, N., Deng, S., Liddelow, S.A., Zhang, C., Daneman, R., Maniatis, T., Barres, B.A., Wu, J.Q., 2014. An RNA-sequencing transcriptome and splicing database of glia, neurons, and vascular cells of the cerebral cortex. *J. Neurosci.* 34, 11929–11947.
- Zhang, Y., Sloan, S.A., Clarke, L.E., Caneda, C., Plaza, C.A., Blumenthal, P.D., Vogel, H., Steinberg, G.K., Edwards, M.S., Li, G., Duncan 3rd, J.A., Cheshire, S.H., Shuer, L.M., Chang, E.F., Grant, G.A., Gephart, M.G., Barres, B.A., 2016. Purification and characterization of progenitor and mature human astrocytes reveals transcriptional and functional differences with mouse. *Neuron* 89, 37–53.
- Zhao, X., Bausano, B., Pike, B.R., Newcomb-Fernandez, J.K., Wang, K.K., Shohami, E., Ringger, N.C., DeFord, S.M., Anderson, D.K., Hayes, R.L., 2001. TNF-alpha stimulates caspase-3 activation and apoptotic cell death in primary septo-hippocampal cultures. *J. Neurosci. Res.* 64, 121–131.
- Zhao, W., Sun, Z., Wang, S., Li, Z., Zheng, L., 2015. Wnt1 participates in inflammation induced by lipopolysaccharide through upregulating scavenger receptor A and NF- κ B. *Inflammation* 38, 1700–1707.
- Ziv, Y., Ron, N., Butovsky, O., Landa, G., Sudai, E., Greenberg, N., Cohen, H., Kipnis, J., Schwartz, M., 2006. Immune cells contribute to the maintenance of neurogenesis and spatial learning abilities in adulthood. *Nat. Neurosci.* 9, 268–275.